Complex Polymer Architectures using Ring-Opening Metathesis Polymerization: Synthesis, Applications, and Practical Considerations

*Sarah E. Blosch, Samantha J. Scannelli, Mohammed Alaboalirat, John B. Matson**

Department of Chemistry and Macromolecules Innovation Institute, Virginia Tech, Blacksburg, Virginia, 24061, United States

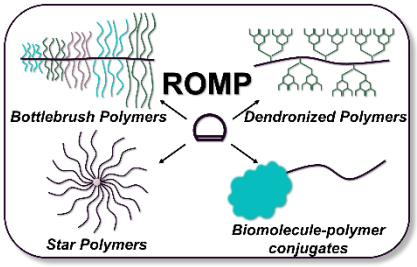

For Table of Contents only

We dedicate this to the late Professor Robert H. Grubbs in honor of his impact in the area of polymer science.

Abstract

Nature shows us that complex molecular architectures lead to unique material properties, and these observations have driven polymer scientists to synthesize complex architectures in an effort to discover how topology influences properties in synthetic polymers. In this Perspective we discuss a variety of complex architectures synthesized using ring-opening metathesis polymerization (ROMP), including multiblock linear polymers, bottlebrush homopolymers and (multi)block copolymers, dendronized polymers, star polymers, and polymer-biomolecule conjugates. Traditional and recently developed synthetic methods including polymerization-induced self-assembly, copolymerization to create gradient structures, and engineering approaches to making complex topologies using ROMP are also reviewed. In this context we highlight emerging applications stemming from these materials, including drug delivery

vehicles, nanoscale constructs, and components in light refraction or energy storage, among others. Finally, we conclude with an in-depth discussion on practical considerations in ROMP that enable the highest level of control when synthesizing complex polymer topologies from sterically demanding or otherwise challenging (macro)monomers. Our hope is that this Perspective will guide scientists synthesizing complex polymer architectures toward new and innovative materials with the potential for unique properties and applications.

1. Introduction

Polymers with non-linear architectures (topologies) have fascinated polymer scientists for decades and continue to do so well into the 21st century. Interest in this field is driven largely by the opportunity for complex polymer architectures to reveal how topological changes influence properties. Fundamental questions include how the star architecture influences crystallinity, how lack of entanglements in densely grafted comb polymers (aka, bottlebrush polymers) influences elasticity, and how block copolymer topology influences phase diagrams. These questions are inspired in part by complex polymer architectures that appear in nature, such as many proteoglycans (comb or bottlebrush). In these complex biopolymers, polymer architecture drives function, and polymer scientists aim to follow nature's blueprints to study how synthetic polymers with complex architectures can afford properties and functions inaccessible in linear polymers. However, before new properties and applications can be manifested, precise methods for controlled synthesis of complex polymer architectures are needed.

Early efforts to synthesize polymers with complex architectures focused on comb polymers and star polymers, where a comb polymer contains linear chains emanating from a main chain (sometimes called a backbone chain) and a star polymer is composed of linear chains (arms) emanating from a single branch point.[1] Houtz and Adkins were the first to detect the presence of comb polymers in 1933 when they polymerized styrene in the presence of polystyrene and observed an increase in viscosity.[2] A few years later

in 1937, Flory proposed that some vinyl monomers could lead to the formation of polymer grafts through chain transfer to polymer reactions, explaining the phenomenon observed by Houtz and Adkins.[3] In 1950 at an ACS meeting, Bandel and Alfrey[4] introduced the idea of graft copolymerization, i.e., a chemically distinct backbone and side chains, with their discovery that vinyl acetate polymerizes in the presence of styrene-vinylidene chloride copolymers to create a graft copolymer.[5] Star polymers first appeared in 1948 when Schaefgen and Flory reported the first systematic study of 4- and 8-arm poly(caprolactam) star polymers made using core molecules containing 4 or 8 carboxylic acid units, respectively.[6] This landmark study showed that rational molecular design could be applied to synthesize star polymers with well-defined numbers of arms without crosslinking. Overall, these early efforts laid the groundwork for the complex polymer topologies we know today.

Although methods have existed to synthesize complex polymer architectures for the better part of a century, only in the past few decades has it become possible to synthesize them with a wide range of monomer types and a high level of control over molecular weights, end-group functionalities, and (multi)block structures. Precise structural control has begun to enable careful studies on structure-property relationships. This synthetic success has relied largely on living or controlled polymerization methods, including anionic polymerization, various reversible deactivation radical polymerization (RDRP) methods [primarily nitroxide-mediated radical polymerization (NMRP), atom-transfer radical polymerization (ATRP), and reversible addition-fragmentation chain transfer (RAFT) polymerization], ring-opening polymerization (ROP), and ring-opening metathesis polymerization (ROMP). In many cases, two or more of these polymerization methods can be combined for rapid synthetic access to complex polymer topologies, sometimes in one pot, eliminating the need for any protection/deprotection schemes.

In this Perspective, we focus on the role of ROMP in making complex polymer topologies. These include (multi)block copolymers, star polymers, biomolecule-polymer conjugates, graft/comb/bottlebrush polymers, dendronized polymers, and other related topologies. We do not discuss cyclic polymers made by ring-expansion metathesis polymerization (REMP),[7] which is related to ROMP but fundamentally different

because the catalysts employed must be designed for REMP to enable both polymer growth and extrusion of the cyclic products. While ROMP is not the only method to make complex polymer topologies, it often has advantages over other methods, such as increased air, water, and functional group tolerance compared with anionic polymerization and a lack of concern for polymer–polymer coupling reactions as can occur in RDRP techniques. We also discuss emerging synthetic strategies, for example, methods where a change in topology occurs, termed macromolecular metamorphosis. Some current and envisioned applications of these polymers are also briefly detailed. Throughout, we discuss how specific choices influence the structure and purity in the final polymer product, including choice of catalyst, monomer type, solvent, and other design or reaction parameters. Finally, we summarize these findings in a section focusing specifically on practical considerations.

2. ROMP Catalysts

ROMP is a polymerization method that is typically driven by the relief of ring strain in cyclic olefin monomers[8] or in some cases by entropy for very large, unstrained cyclic olefins.[9] The most common ROMP catalysts are the Ru complexes developed by Grubbs (Figure 1A-D) and the primarily Mo-based catalysts introduced by Schrock (Figure 1E). All of these catalysts are transition metal complexes that contain a carbon–metal double bond. We note that these transition metal (pre)catalysts may be more accurately referred to as ROMP initiators in many contexts, but we use the more common term catalyst throughout for sake of ease, clarity, and in an attempt to reduce potential confusion. The main practical distinction between these two main classes of catalysts is that the Mo catalysts are somewhat more active, but they are limited by air and moisture sensitivity and react with some common functional groups. In contrast, the Grubbs' catalysts are generally bench stable and tolerate air and water. Additionally, these Ru catalysts have specificity for the C=C bond, which allows for polymerization of monomers with pendant functional groups that often cannot be polymerized by other methods (i.e., those that are sensitive to radicals or anions).

Due to this high functional group tolerance and ease of handling, the Grubbs' catalysts are used widely in ROMP. Of these, Grubbs' 3rd generation catalyst [G3, $(H_2IMes)(Cl)_2(pyr)_2RuCHPh$] is most commonly used in the synthesis of complex polymer architectures by ROMP due to its fast initiation and propagation kinetics.[10] G3 is the catalyst used in many of the examples discussed here. Either unsubstituted pyridine ligands can be used, or they can be substituted at the 3-position with a halogen, usually Br. Here we do not distinguish between unsubstituted and halogen-substituted versions of G3, referring to both types simply as G3. The G3 catalyst can be easily prepared from commercially available Grubbs 2nd generation catalyst [G2, $(H_2IMes)(Cl)_2(PCy_3)RuCHPh$] by treatment with pyridine or a substituted pyridine.[11,12] G2 is itself not typically used in ROMP when living characteristics are needed due to its slow initiation compared to propagation rate; Hoveyda-Grubbs G2 catalyst [HG2, $(H_2IMes)(Cl)_2(o\text{-}OiPrC_6H_4)RuCHPh$] exhibits similarly slow initiation.[13] Grubbs 1st generation catalyst [G1, $(PCy_3)_2(Cl)_2RuCHPh$] is also used to some extent to make complex polymer architectures by ROMP because it also exhibits fast initiation related to propagation, enabling living characteristics. However, G1 propagates a few orders of magnitude slower than G2/G3 catalysts.[14]

Beyond catalysts capable of mediating ROMP with living characteristics, there exist ROMP catalysts capable of controlling *cis*/*trans* stereochemistry in the resulting polymer. Some catalysts can also control tacticity in ROMP. Many of these catalysts are based on Mo or W transition metals, although some Ru-based catalysts with control over polymer microstructure have been developed. These topics were recently reviewed by Buchmeiser.[15] In figures here we do not intend to imply control over backbone olefin stereochemistry. Attributes of specific catalysts are discussed in further detail in the Practical Considerations section.

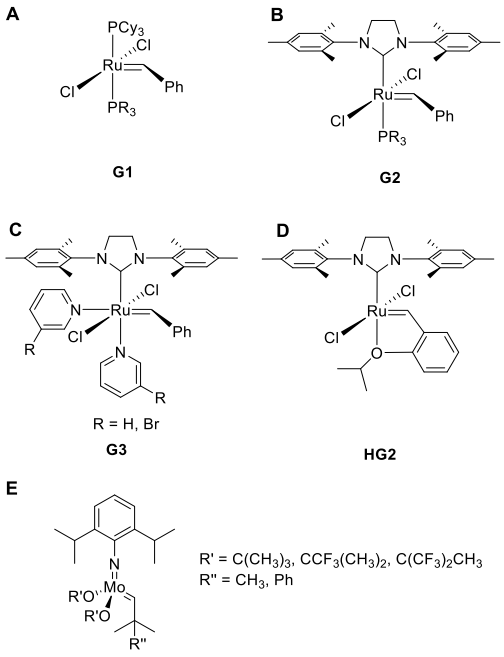

Figure 1. Commonly used catalysts for ROMP A) Grubbs' 1st generation (G1), B) Grubbs' 2nd generation (G2), C) Grubbs' 3rd generation (G3), D) Hoveyda-Grubbs' 2nd generation (HG2), and E) Schrock Mo-based catalysts.

3. Block and Multiblock Copolymers

Block copolymers (BCPs) have been investigated extensively since their introduction in the early 1950s.[16] Most BCPs to date have been made using anionic or RDRP methods using vinyl monomers. An advantage of using ROMP for the synthesis of BCPs is the straightforward functionalization of strained cyclic olefin monomers such as norbornenes coupled with the high functional group tolerance of ROMP.[14] Synthesizing BCPs and multiblock (i.e., those with more than 2 blocks) copolymers via ROMP is operationally simple because each monomer can be consecutively polymerized to full conversion, avoiding intermediate workup steps that are required in most RDRP BCP syntheses. BCP synthesis by ROMP dates back to the 1990s using Ru- and Mo-based catalysts and has been reviewed recently.[17] ROMP can also be paired with other polymerization techniques, such as silyl aldol condensation polymerization as early as the late 1980s,[18] and more recently ATRP, RAFT, or ROP, to create BCPs and multiblock copolymers from different monomer classes.[19–21]

While BCP synthesis via ROMP is relatively straightforward, catalyst death (the main form of chain termination in ROMP), makes the preparation of triblock, tetrablock, or higher multiblock copolymers challenging. The catalyst death is a result of the monomer-starved conditions that occur as monomer concentration drops toward the end of each block addition, increasing the polymerization time, allowing for catalyst decomposition.[22] Regardless of these challenges, synthesis of BCPs and multiblock copolymers by ROMP has enabled the creation of unique polymer structures, supramolecular aggregates, and applications.[23]

3.1 Linear multiblock copolymers

Triblock copolymers have been synthesized using ROMP to achieve telechelic materials for achieving specific endgroups.[24] Kilbinger and coworkers developed a strategy for synthesizing these difunctional telechelic polymers with low dispersities using ROMP and termed the method "sacrificial synthesis".[25] This synthetic technique involves chain-extending a polymer with a polymer block that is eventually cleaved, or sacrificed, to leave a specific end group on the first polymer. Their first example of sacrificial synthesis involved BCP synthesis by chain extending a poly(*exo*-*N*-phenylnorbornene-2,3-dicarboximide) (PNI) with a dioxepine monomer (a 7-membered cyclic olefin containing a degradable acetal linkage). The poly(dioxepine) block in the resulting diblock copolymer was sacrificed via acid-catalyzed degradation of the acetal units to leave a single hydroxyl group attached to the PNI homopolymer ω chain end, which was used to install a number of different functional groups onto the PNI chain end (Figure 2A). While this method enabled simple functionalization of the ω end of the PNI homopolymer, the α chain end remained a phenyl group left behind from initiation with the ruthenium catalyst. In follow-up work, Kilbinger and coworkers made an ABA triblock copolymer of the structure poly(dioxepine)-*b*-PNI-*b*-poly(dioxepine) with two different types of poly(dioxepines) cleavable under different conditions.[24] Sequential degradation of the poly(dioxepine) blocks followed by chain end modification reactions allowed them to tune both of the PNI chain ends independently (Figure 2B). While this method was successful, a drawback was the consumption of one equivalent of catalyst for every telechelic PNI chain. The authors found that if they

synthesized ABABA pentablock or even ABABABA heptablock copolymers with alternating poly(dioxepine) and PNI blocks, followed by acid hydrolysis, they could synthesize two or even three telechelic PNIs per equivalent of catalyst.

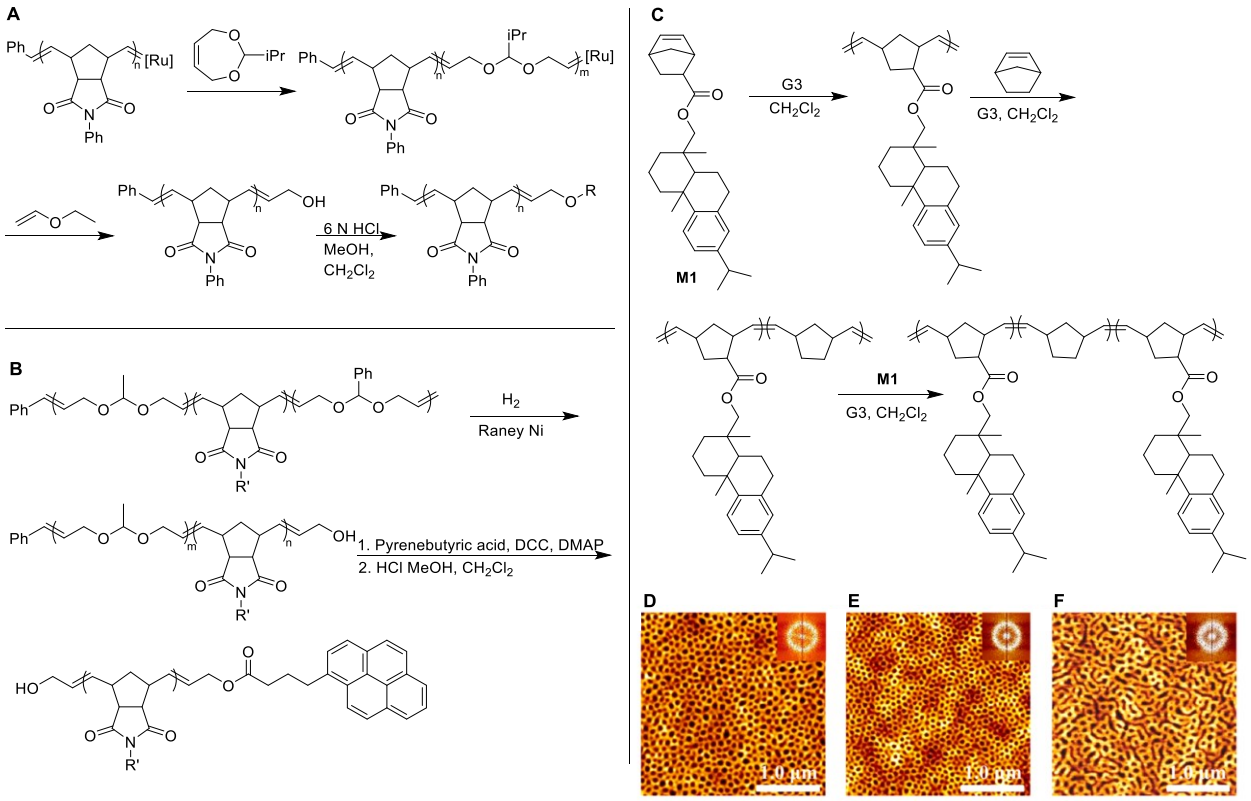

Figure 2. Synthesis of A) Di- and B) ABC triblock polymers by ROMP to create telechelic polymers via sacrificial synthesis. C) Synthetic scheme for ABA triblock copolymer synthesis, D-F) atomic force microscopy (AFM) images of microphase separated films created by ABA triblock copolymers for different block molecular weights. Adapted with permission from references [24–26].

The synthesis of multiblock copolymers by ROMP is not limited to sacrificial synthesis. An early example of multiblock copolymer synthesis by ROMP reported in 2004 involved the polymerization of norbornene monomers containing acetyl-protected carbohydrates.[27] In this work, G1 catalyst mediated the synthesis of tetrablock copolymers with high conversions and low dispersities (usually within the range of 1.10-1.20), although block lengths were generally small with overall molecular weights limited to ~30 kg/mol. Astruc

and coworkers took a similar approach, using G3 catalyst to initiate the polymerization of multiple different monomers in sequence to make electrochromic triblock and tetrablock copolymers with side-chain metallocene units.[28,29] Recently, Tang and coworkers reported the synthesis of tri- and pentablock copolymers with high molecular weights using sequential ROMP to create tough bioplastic films.[26] Here, G3 catalyst was used to prepare ABA and ABABA copolymers from a dehydroabietic acid-derived norbornene monomer (natural rosin functionalized with a norbornene unit, shown in Figure 2C) and norbornene. Molecular weights ranged from 100–200 kg/mol, and these copolymers created microphase-separated materials that were molded into stiff yet tough films (Figure 2D-F). This example highlights how ROMP can be used to synthesize well-defined multiblock linear copolymers from renewable sources that exhibit microphase separation, leading to high toughness that is difficult to achieve in many bio-derived polymers.

3.2 Ring-opening metathesis polymerization-induced self-assembly

Polymer-induced self-assembly (PISA) is a method of producing BCP nanomaterials with high solids contents (often >10%) that avoids isolation and dialysis steps traditionally required in making these materials. This process begins with a homopolymer that is chain-extended with a second monomer and is highly dependent on the solubility of this second monomer and its polymer in the chosen solvent in this chain-extension step. The original homopolymer is soluble in the solvent, as is the monomer for the chain-extension step; however, as the second monomer polymerizes, the polymer becomes insoluble in the solvent, driving self-assembly into nanostructures.[30] RDRPs are often used for PISA, specifically RAFT as it offers an extensive breadth of functional monomers.[31–33] In the past decade, ring-opening metathesis polymerization-induced self-assembly (ROMPISA) has been implemented to complement RAFT PISA approaches. Unlike traditional PISA by RAFT, ROMPISA allows for materials that can be synthesized at room temperature under air while also incorporating complex monomers.[34] Additionally, ROMPISA can be carried out using backbone chemistries that could not be implemented using traditional RAFT or other radical strategies (i.e., degradable linkages).[35]

ROMPISA was first introduced as an *in situ* polymerization method in 2010.[36] G1 catalyst mediated the polymerization of a norbornene monomer to make a homopolymer that was soluble in toluene; next, an oxanorbornene monomer that was soluble in toluene was added, forming a block copolymer with a toluene-soluble polynorbornene (PNb) block and a toluene-insoluble polyoxanorbornene (PONb) block. Using this one-pot ROMPISA strategy, nanospheres ranging in size from 136 to 210 nm were synthesized. This work paved a path for synthesizing more complex BCP assemblies by ROMPPISA. For example, Choi and coworkers used ROMPISA to make self-assembled, semi-conducting "nanocaterpillars" containing a polyacetylene core block and a PNb outer soluble block.[37] These materials were created by first polymerizing a norbornene monomer in CH_2Cl_2 then chain extending with cyclooctatetraene using G3 catalyst. The formation of the "nanocaterpillar" morphology, which resembles a string of pearls, was attributed to the π-π interactions in the polyacetylene block. A major advantage of ~~the~~ using ROMPISA ~~approach~~ here was that it limited the depolymerization of polyacetylene to form benzene, a problem commonly encountered in ROMP approaches to make this structurally simple but unstable conjugated polymer.

Early research on ROMPISA was performed in nonpolar solvents, but more recently, advances in ROMPISA using polar solvents have been achieved in efforts to make nanostructures with applications in biomedicine. Gianneschi and coworkers utilized a norbornenyl oligo-(ethylene glycol) monomer to form the soluble block and a norbornene-capped protected peptide as the monomer to form the insoluble, chain-extended polymer in a ROMPISA approach (Figure 3).[34] Solvent studies revealed that a mixture of dimethylformamide and methanol in a ratio of 1:2 was ideal for this PISA synthesis to form a variety of nanostructures depending on the length of the peptide-containing block.

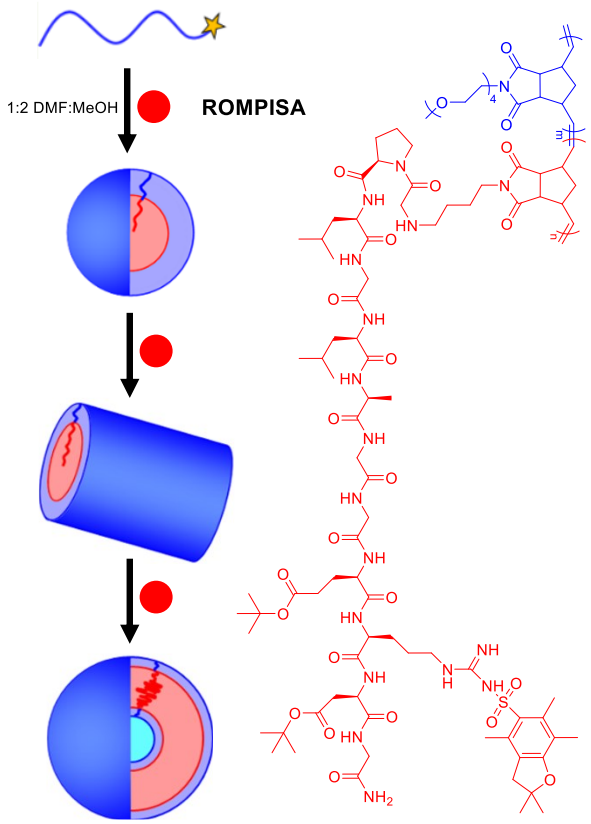

Figure 3. Schematic illustration of ROMPISA using a polymer peptide amphiphile. The polymer blue is hydrophilic while the red polymer is a hydrophobic polymer with a pendant peptide. Adapted with permission from reference [34].

The ultimate goal in PISA for biological applications is to conduct the polymerization entirely in water. In the case of ROMPISA, this is difficult due to the insolubility and low activity of most ROMP catalysts in water. Gianneschi and coworkers addressed this problem by using a water-soluble, quaternary amine-based HG2-type second-generation catalyst.[38] In this work, a charged, norbornene-capped peptide was used to make the water-soluble block, followed by chain-extension with a quaternary amine-based phenyl norbornene dicarboximide to make the water-insoluble block. The final block copolymer formed spheres for shorter peptide chain lengths and vesicles for larger peptide chain lengths, and cleavage of part of the peptide sequence using the proteolytic enzyme thermolysin led to the formation of larger aggregates. A related aqueous ROMPISA strategy was applied by the same group to make cisplatin-loaded nanoparticles

that displayed cytotoxicity behavior toward human ovarian and cervical cancers.[39] Finally, O'Reilly and coworkers have addressed the catalyst solubility problem by first preparing a water-soluble PNb block in organic solvent using the G3 catalyst, then transitioning the water-soluble PNb block into water, with the catalyst still on the chain end, to make the water-insoluble block.[40] They also discovered that controlling the concentration of Cl^- can increase control over the polymerization, leading to higher conversion in the aqueous ROMP step.[41] As evidenced by the recent work, ROMPISA is a new field that broadens the outlook for potential nanostructures, applications, and capabilities of ROMP.

4. Bottlebrush homopolymers

Bottlebrush polymers, also termed molecular brushes, are graft polymers with densely grafted side chains attached to a linear polymer backbone.[42–44] Many polymerization techniques are suitable for the synthesis of bottlebrush polymer backbones, side chains, or both, using the synthetic strategies detailed below. Historically, anionic polymerization was preferred because it enabled precise control over molecular weight and end group functionality needed to make bottlebrush polymers.[45] More recently, RDRP techniques as well as ROP and ROMP methods have gained popularity in bottlebrush polymer synthesis. In many cases, more than one type of polymerization technique is used. The general goal is to synthesize bottlebrush polymers with tunable chemical composition, controllable and high grafting density, and tunable side chain and backbone degrees of polymerization (N_{sc} and N_{bb}, respectively). The dense packing and steric repulsion of polymer side chains along the backbone hinders entanglement and forces extension of the backbone chain, forming stiff cylindrical nanostructures in many cases.[46] The high molecular weight but unentangled nature of bottlebrush polymers generates interesting mechanical and rheological properties, which are altered by the composition and the N_{sc} and N_{bb} of the bottlebrush polymer.[47]

There exist four general strategies to synthesize bottlebrush polymers, grafting-to, grafting-from, transfer-to, and grafting-through, which differ in how the side chains are connected to the backbone chain.[48] Grafting-to requires separate polymerization reactions to generate the backbone and the side chains,

followed by efficient reactions to attach the side chains to the backbone. The grafting-from method requires the polymerization of a monomer with a pendant functional group to make the backbone chain. Next, initiation sites are attached to the backbone (if they were not already pre-installed on the monomer), which are then used in a subsequent polymerization step to initiate the synthesis of the sidechains. The transfer-to strategy is a hybrid of grafting-to and grafting-from that is less widely used. It involves the synthesis of a polymer backbone with a pendant chain transfer agent attached via the Z-group in the case of RAFT. The side chains are synthesized in a process where propagation occurs free in solution, and the growing side chains return to the backbone via a chain transfer reaction.[49] Lastly, the grafting-through method involves the synthesis of a monotelechelic polymer with a polymerizable group on one chain end, called a macromonomer (MM). Polymerization of the MM end-groups creates the bottlebrush polymer backbone in a second step. While all four methods have advantages and disadvantages and various potential side products, grafting-through holds the potential for the greatest level of control over grafting density, N_{sc}, and N_{bb}. Although ROMP can be used in all four methods, it is most commonly applied in the grafting-through of MMs, with early reports from Bowden in 2004,[50] and later Grubbs in 2009,[51] highlighting the capability of ROMP grafting-through to make long cylindrical bottlebrush polymers. ROMP has advantages in the polymerization of MMs over the RDRP methods, which can be hampered by low equilibrium monomer concentrations under standard conditions, even using low molecular weight macromonomers.[52] In this section we discuss the use of ROMP in making bottlebrush homopolymers using the grafting-through method, focusing on how different approaches to MM synthesis influence the purity of the ultimate bottlebrush polymer product.

4.1 Direct-growth vs. growth-then-coupling

ROMP grafting-through involves the polymerization of MMs, which are made using controlled or living polymerization techniques. MMs used in ROMP grafting-through most often contain a norbornene functional group due to its high ring strain and fast polymerization by ROMP. Here we discuss norbornene-based MMs for the sake of simplicity, but other strained cyclic olefins have been used as well. The release

of ring strain in the norbornene unit provides the driving force for the polymerization, and fast initiation rates and even faster propagation rates in ROMP can afford bottlebrush polymers in minutes.[10] The norbornene groups can be present during side chain synthesis or added in a post-polymerization modification reaction, and these approaches are referred to as direct-growth and growth-then-coupling, respectively (Figure 4).[53]

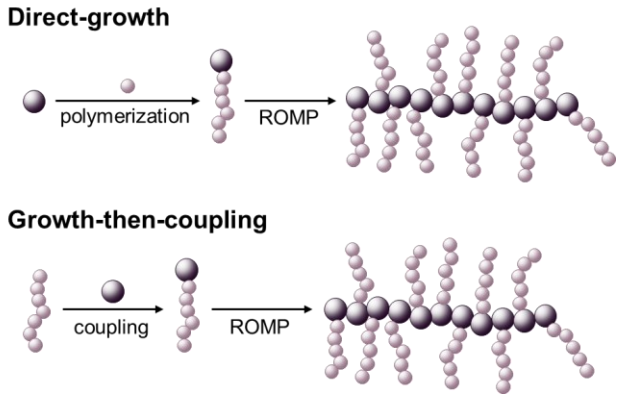

Figure 4. Schematic representation of bottlebrush polymer synthesis via the direct-growth and growth-then-coupling strategies.

Direct-growth is most commonly used in making bottlebrush polymers due to the more straightforward synthetic approach. This method relies on the use of a norbornene functionalized with an initiator or chain transfer agent for a different polymerization technique, often ROP or an RDRP technique. Polymerization is carried out from this norbornene-functionalized unit to generate an MM, and then ROMP is used in the second step to form the backbone without any modification. The MM is typically isolated before the ROMP reaction, but one-pot syntheses using the direct-growth method are possible, as detailed below. Bowden and coworkers were the first to synthesize bottlebrush polymers using ROMP in the direct-growth method, achieving narrowly disperse polymers with molecular weights exceeding 60,000 kg/mol.[54,55] Since then, others have been able to successfully achieve large degrees of polymerization of the backbone using this method, although such enormous molecular weights remain difficult to access for most MMs.

RDRPs are typically used to make MMs to ensure low dispersities and the high chain end fidelity necessary for the subsequent ROMP step. A variety of dual-functionalized small molecules have been made that carry a norbornene (or similar) unit and an initiator or chain-transfer agent (CTA) for the RDRP step. The RDRP techniques most commonly used to make MMs are ATRP[56] and RAFT.[57] With these techniques, MMs of polystyrene (PS), poly(methyl methacrylate) (PMMA), poly(methyl acrylate) (PMA),[58] poly(*tert*-butyl acrylate) (PtBA),[59] and poly(*N*-isopropylacrylamide)[60] have been made and used to synthesize bottlebrush polymers via ROMP. In one of the first reports on this topic in 2006, Patton and Advincula showed that the direct-growth method enabled the synthesis of well-defined PS and PMMA MMs using a combination of RAFT and ROMP, with efficient ROMP to generate small BB polymers (N_{bb} = 8).[58]

One important consideration in the synthesis of BB polymers using the direct-growth approach is the potential for copolymerization of the norbornene unit in the RDRP reaction. For example, some studies have shown bimodal MW distributions for the resulting bottlebrush polymers, specifically those where polyacrylates were prepared in the RDRP step.[56,58,61] Xia and Grubbs noticed this problem in 2009 in the synthesis of MMs using both ATRP and RAFT of acrylates, suggesting that the norbornene can interfere with the initial polymerization of the sidechain.[51] Keddie and coworkers recently reported a systematic study on this problem and suggest some methods to limit it, such as running RDRP reactions to low monomer conversion.[61] However, to avoid this problem entirely, the growth-then-coupling method can be used.

Initially used as early as 1994 by Feast and coworkers with Mo-based catalysts[62] and later coined by Xia in 2015,[53] the growth-then-coupling method involves the synthesis of the side chains followed by a chain end modification reaction to install the norbornene unit (Figure 5). Although the growth-then-coupling approach lengthens the synthesis with the addition of intermediate reactions and purification steps, it removes any interference of the sidechain polymerization with the norbornene unit, allowing for the synthesis of well-defined bottlebrush polymers.[51] This synthetic strategy can accommodate a broader scope of monomers and

polymerization techniques than the direct-growth strategy but is limited by the intermediate modification step.

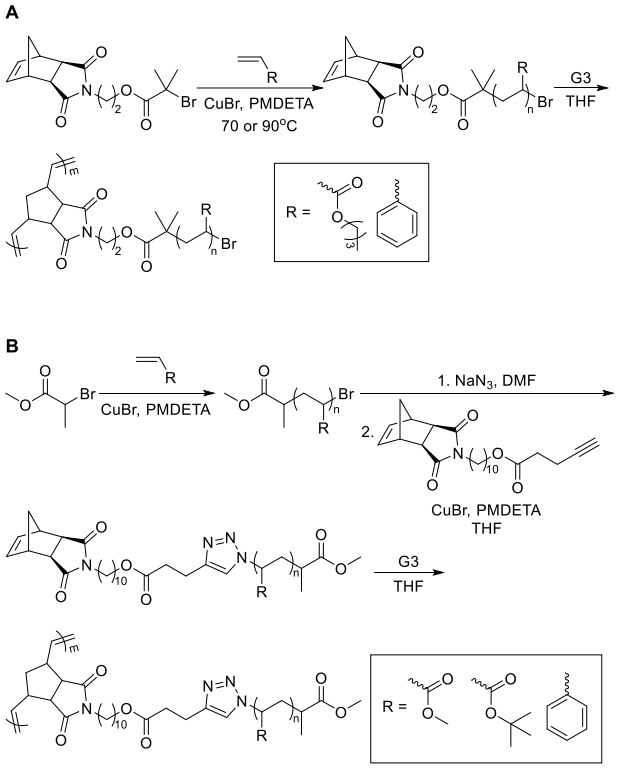

Figure 5. Synthesis of various MMs via the A) direct-growth and B) growth-then-coupling approaches. Adapted with permission from references [51,53].

In order for the growth-then-coupling strategy to be successful, highly efficient intermediate reactions need to be used to ensure full functionalization of the sidechains, which typically include "click" reactions[53] or carbodiimide couplings.[63] Anionic polymerization, RAFT, ATRP, and ROP have been used to polymerize well-defined side chains of PMA, PtBA, PS,[51] PMMA,[53] polycaprolactone, and poly(ethylene oxide) (PEO)[63] with one end group capable of further reaction. A high-yielding coupling reaction, potentially followed by purification, enables the synthesis of the MM. If done correctly, the growth-then-coupling strategy ensures bottlebrush polymer formation via grafting-through without branching. However, care must be taken to confirm that MMs are fully functionalized with a norbornene or similar unit; MMs lacking

a polymerizable unit are simply side chains that do not attach to the backbone in the grafting-through step. Ultimately, assuming high purity MMs in both cases, when comparing identical MMs made by the direct-growth and growth-then-coupling approaches, those made by growth-then-coupling achieve bottlebrush polymers of higher molecular weight and lower dispersity than those made by direct-growth.[53]

4.2 Purity Considerations

As alluded to above, an important factor to consider when performing the grafting-through method is the intermediate purification of the MM, which tends to be extensive. For direct-growth, these purifications generally include multiple precipitation steps to remove residual monomer, requiring large amounts of solvent and are tedious for polymers with low glass transition temperatures (T_g's). If vinyl monomers are used to make the MM, exhaustive removal is usually required because even very small amounts of residual monomers such as acrylates can act as chain transfer agents or terminators in ROMP, especially when targeting large DPs or when making bottlebrush polymers using the grafting-through process.[64] In addition to precipitation steps and residual monomer removal, growth-then-coupling also requires purification after the post-polymerization modification reaction to attach the norbornene. Removal of residual impurities from previous reactions is crucial in order to achieve bottlebrush polymers of high MW and low dispersity. Even after exhaustive removal of any vinyl monomer, small amounts of other impurities (e.g., alkynes) can be detrimental in the ROMP step due to the small amount of catalyst needed in comparison to the MM. Bang and coworkers investigated how residual impurities in MMs made via "click" reactions through the growth-then-coupling method affected ROMP.[65] They observed higher conversion and lower dispersities for MMs that were rigorously purified compared to MMs with residual impurities, confirming the importance of purity to produce well-defined bottlebrush polymers.

Although impurities can be detrimental to the ROMP step of the grafting-through method, several groups have avoided this problem in developing one-pot syntheses of bottlebrush polymers. One-pot processes simplify the synthesis of bottlebrush polymers by removing intermediate purification steps, although they

are limited in scope. The first attempt at a one-pot bottlebrush polymer synthesis by ROMP grafting-through was in 2009 by Cheng and coworkers,[66] but was reported as uncontrolled with large dispersities compared to a similar grafting-from one-pot method. A successful attempt at a one-pot synthesis was performed in 2012 by Wooley and coworkers using RAFT to make a PMMA MM followed by ROMP with an intermediate cooling step to quench the RAFT reaction (Figure 6).[67] This synthesis was successful despite residual vinyl monomer because MMA does not react with Grubbs' catalysts,[68] but most other vinyl monomers are metathesis active and therefore cannot be easily used in one-pot syntheses. To broaden the scope of monomers available for a one-step procedure, our group used ROP to make MMs of poly(lactic acid) (PLA) followed by ROMP. The choice of a 1,8-diazabicyclo[5.4.0]undec-7-ene (DBU) cocatalyst system for the ROP step based on its ability to maintain high end group fidelity enabled a high degree of control over the ROP, creating MMs of low dispersity and only required the addition of trifluoroacetic acid to terminate the ROP step before moving forward with the ROMP step.[69] Klapper and coworkers recently extended this ROP/ROMP concept to make BB polymers using a simultaneous polymerization approach, where the ROP and ROMP steps can occur in the same pot at the same time in a hybrid of grafting-through and grafting-from.[70]

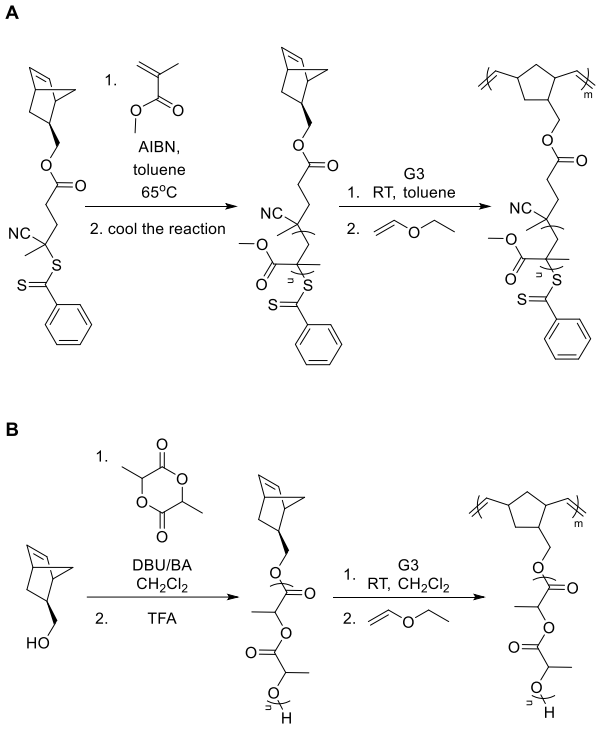

Figure 6. Synthesis of bottlebrush polymers with (A) PMMA side chains and (B) PLAside chains via a one-pot method. Adapted with permission from references [67,69].

5. Bottlebrush (Multi)Block Copolymers

5.1 Diblock and triblock bottlebrush BCPs

Along with bottlebrush homopolymers, ROMP enables the synthesis of bottlebrush BCPs, adding another dimension of complexity to this topology. Bowden and coworkers reported the first synthesis of a series of BCPs that included one linear block and one bottlebrush block (i.e., linear-*block*-bottlebrush copolymers) in a pair of reports in 2007 and 2008.[55,71] In a large systematic study of 32 polymers, they highlighted how N_{bb} and N_{sc} of the bottlebrush component and the DP of the linear component influenced solid-state morphology.[55] Grubbs and coworkers reported the first synthesis of a bottlebrush BCP with two bottlebrush blocks by ROMP in 2009.[72] In this work, the growth-then-coupling method was used for the preparation of PS, PtBA, and poly(*n*-butyl acrylate) (PnBA) MMs, which were synthesized using ATRP followed by

coupling a norbornene to the MM chain end, while a PLA MM was synthesized using the direct-growth method. A series of bottlebrush BCPs were then prepared using sequential ROMP of different combinations of two MMs (Figure 7A). This method enabled the synthesis of a variety of bottlebrush BCPs with variable side chain chemistry, N_{sc}, and N_{bb} values. Small-angle X-ray scattering (SAXS) and AFM studies on these polymers showed self-assembly as evidenced by a bright green color due to the reflectance of light from the nanosized self-assembled domains (Figure 7B).

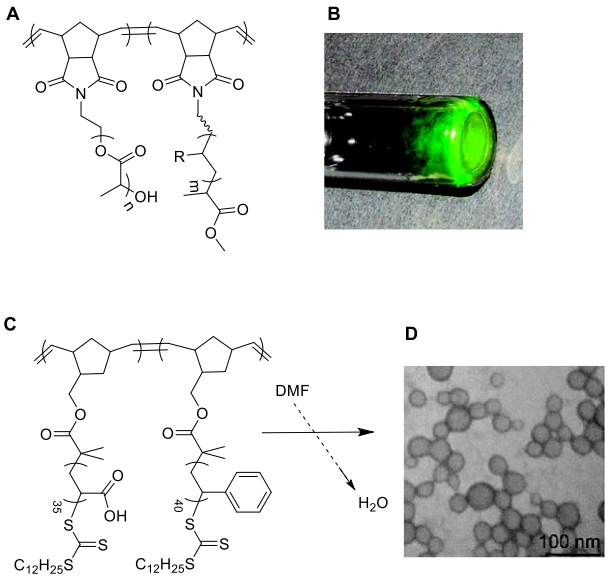

Figure 7. (A) Chemical structure of bottlebrush BCP based on PLA, PtBA, and PnBA side chains. (B) Photograph of bottlebrush BCP after drying showing green color due to reflectance from the large self-assembled domains. (C) Synthesis of bottlebrush BCP based on PAA and PS side chains. (D) TEM image of self-assembled bottlebrush BCP in aqueous solution into micelles. Adapted with permission from references [72,73].

In related work, Wooley and coworkers synthesized bottlebrush BCPs using PS and PtBA MMs prepared by RAFT polymerization. Sequential ROMP afforded a bottlebrush BCP of the structure (PNb-*graft*-PS)-*block*-(PNb-*graft*-PtBA). Hydrolysis of the *tert*-butyl esters in the PtBA side chains afforded an amphiphilic bottlebrush BCP of the structure (PNb-*graft*-PS)-*block*-(PNb-*graft*-PAA), where PAA = poly(acrylic acid) (Figure 7C). These polymers self-assembled in aqueous solution, forming micellar structures (Figure 7D).[73]

The versatility of ROMP grafting-through enables the preparation of bottlebrush multiblock copolymers. The same principle of using sequential polymerizations can be utilized to prepare ABA or ABC triblock or even ABCD tetrablock copolymers, where a PNb backbone is typically used while the variation occurs on the side chains. For example, Wooley and coworkers prepared two different types of ABC bottlebrush triblock copolymers using the grafting-through method with the structures (PNb-*graft*-PEG)-*block*-(PNb-*graft*-PLA)-*block*-(PNb-*graft*-PBAEAM) (B1 and B2) and (PNb-*graft*-PEG)-*block*-(PNb-*graft*-(PHS-*co*-PNPM))-*block*-(PNb-*graft*-PBAEAM) (B3), where PBAEAM = poly(*N*-*tert*-butyloxycarbonyl-*N*′-acryl-1,2-diamino-ethane) and PHS-*co*-PNPM = poly(*p*-hydroxystyrene-*co*-*N*-phenylmaleimide) (Figure 8).[74] Removal of the Boc groups on the PBAEAM side chains afforded a cationic, water-soluble side chain. The self-assembly of these triblock copolymers in aqueous solutions exhibited micellar or vesicular structures.

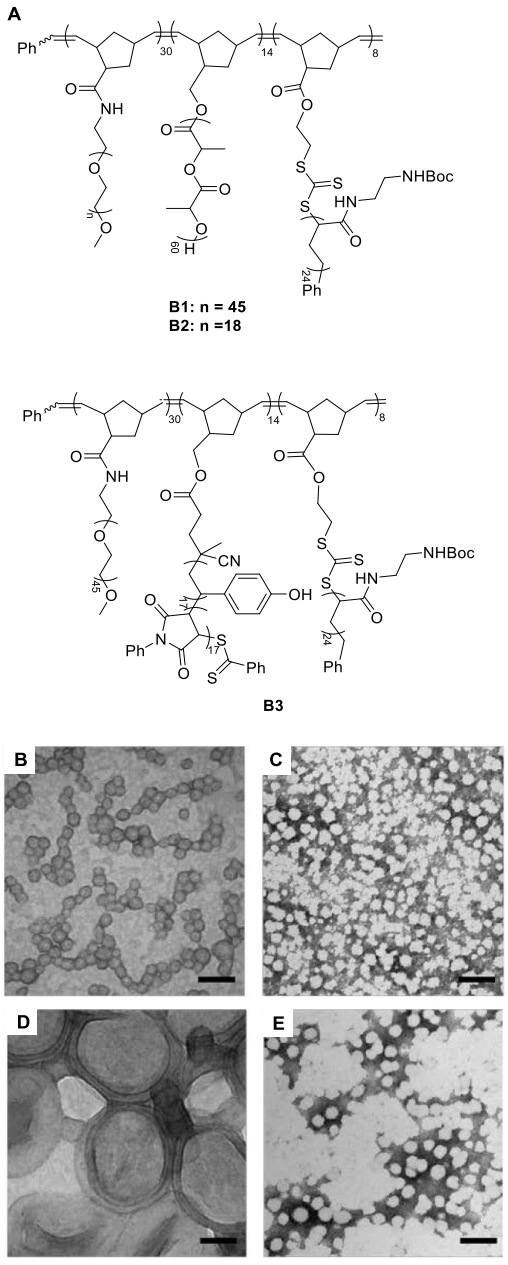

Figure 8. (A) Chemical structures of ABC triblock copolymers. TEM images of self-assembly in aqueous solution of (B) B1 protected with Boc (C) B1 with Boc removed (D) B2 protected with Boc (E) B2 with Boc removed. All scale bars are equal to 100 nm. Adapted with permission from reference [74].

5.2 Core-shell bottlebrush BCPs

Beyond the block copolymers discussed above, another type of bottlebrush BCP is a core-shell bottlebrush BCP. In this case, the macromonomer is a BCP or triblock copolymer with a norbornene on one end. ROMP grafting-through of this type of MM results in a core-shell structure or core-shell-corona structure. A particularly interesting example by Rzayev and Onbulak involved the preparation of core-shell bottlebrush triblock copolymer where the inner block consisted of PLA, the middle block consisted of poly(*tert*-butyl methacrylate) (PtBMA), and the outer block was a statistical copolymer of the structure POEGMA-*stat*-PCEM where POEGMA = poly(oligoethyleneglycol methacrylate) and PCEM = poly(coumarin ethyl methacrylate) (Figure 9A).[75] Once in solution, UV light was used to crosslink the coumarin groups in the corona. Aqueous NaOH was then added to degrade the PLA inner block to create nanotubes. Finally, trifluoroacetic acid was added to the polymer to hydrolyze the *tert*-butyl esters to create a PAA shell (middle block). Nanotubes were observed by transmission electron microscopy (TEM) both in CH_2Cl_2 before the hydrolysis steps and in aqueous solution after the hydrolysis steps, and the cylindrical nanostructures were larger in water likely due to hydrogen bonding, which induced end-to-end anisotropic aggregation (Figure 9B-C).

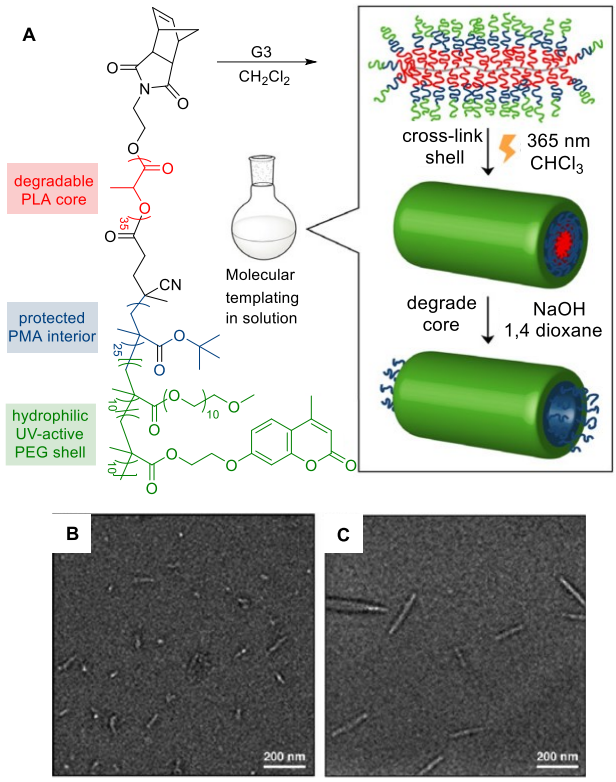

Figure 9. (A) Synthesis of PEG nanotubes with inner functionalities from tricomponent core-shell bottlebrush copolymers. TEM images of core-shell bottlebrush block copolymer (B) PLA degradation and (C) tert-butyl group removal. Adapted with permission from reference [75].

5.3 Janus bottlebrush BCPs

Finally, there is one more type of bottlebrush BPC: Janus bottlebrush BCP synthesis involves ROMP grafting-through of a norbornene connected to two different polymer side chains. Multiple clever methodologies have been used to achieve this type of topology. Johnson and coworkers prepared Janus bottlebrush BCPs using a norbornene-based MM precursor.[76] This precursor contained two orthogonal functional groups, an alkyne for CuAAC coupling and an alcohol for 1-ethyl-3-(3-dimethylaminopropyl) carbodiimide (EDC) coupling. In this example, an azide-functionalized PS MM prepared by ATRP was attached to the norbornene, as well as PLA prepared by ROP. An example of an MM with a clicked PS and

PLA prepared by ROP is shown in Figure 10A. SAXS of these materials revealed that while the Janus MM was disordered, the Janus bottlebrush BCPs were ordered and had bicontinuous gyroid morphology.

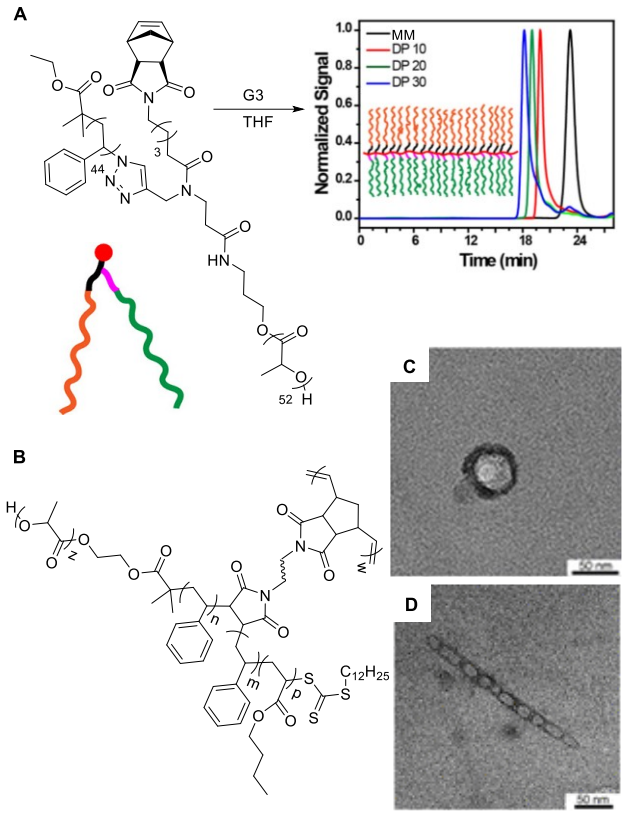

Figure 10. (A) Chemical structure of the norbornene functionalized Janus MM and SEC traces of the MM and resulting bottlebrush polymers at different DPs. (B) Chemical structure of Janus core-shell bottlebrush copolymer. TEM images of Janus core-shell bottlebrush block copolymer in CH_3CN resulting in (C) vesicles (D) a row of vesicles after 7 days of aging. Adapted with permission from references [76,77].

Seo and coworkers prepared an even more complex Janus core-shell bottlebrush block copolymer composed of three types of polymer blocks.[77] Their synthetic method utilized a RAFT chain transfer agent with an alcohol end group, which initiated the polymerization of lactide to make PLA through an ROP step. Next, the authors generated a PS block mediated by the RAFT CTA component. During the synthesis of the PS component, a single unit monomer insertion step was used to introduce a norbornene functionalized maleimide. After the insertion, the RAFT polymerization continued with another PS block and PnBA block. ROMP of this macromonomer with two diblock copolymer side chains (PS-*block*-PLA and PS-*block*-

PnBA) resulted in a bottlebrush block copolymer with both core-shell and Janus structure (Figure 10B). Self-assembly of this Janus core-shell bottlebrush block copolymer in CH_3CN resulted in vesicles as shown by TEM imaging (Figure 10C). After 7 days of aging, the vesicles aggregated into a row of vesicles due to intervesicle adhesion (Figure 10D).

5.4 Engineered Bottlebrush Polymer Structures

Recently, the precision that the grafting-through method by ROMP provides has been exploited to engineer bottlebrush polymers with non-linear and in some cases non-centrosymmetric structures. In other words, the customizability of this method enables the synthesis of bottlebrush polymers where the side chain lengths are varied to generate a targeted shape. A comprehensive example of these types of bottlebrush polymers was demonstrated in a 2019 study published by Guironnet and coworkers where they utilized computer simulations and automated flow synthesis to feed MMs prepared *in situ* immediately into the ROMP reaction.[78] The MMs contained PLA and poly(valerolactone) (PVL) side chains prepared through ROP. The authors conducted the ROP reaction in one reactor and continuously added it to another reactor containing G3 catalyst such that the side chains increased in molecular weight along the polymer backbone, generating a cone-shaped tapered bottlebrush polymer. This methodology was also utilized in another study where PLA and polydimethylsiloxane (PDMS) were utilized as the side chains on the MMs.[79] Further extension of the methodology allowed for even greater control over the molecular geometry of these bottlebrush polymers, with architectures including bowtie, hourglass, and football shapes (Figure 11A). The AFM image of the hourglass shapes is shown in Figure 11B.

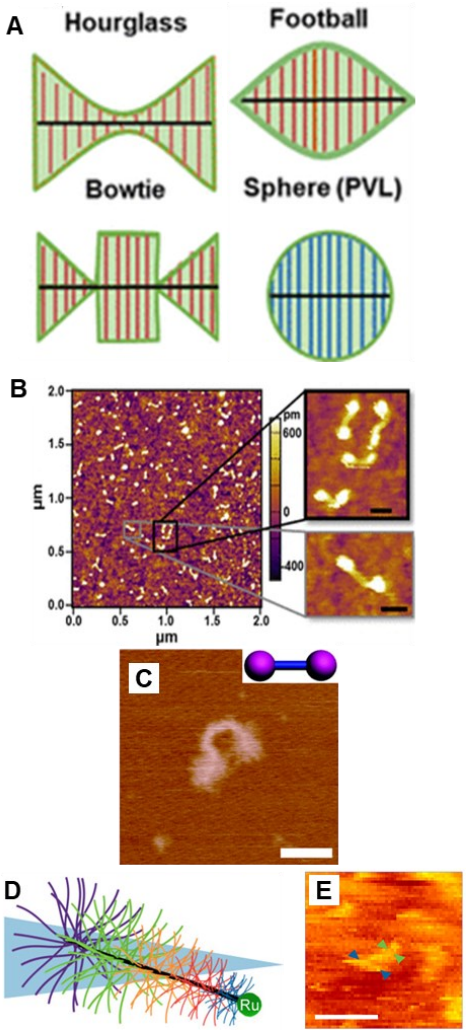

Figure 11. (A) Schematic illustrations of targeted engineered bottlebrush polymers architectures using a continuous flow method. (B) AFM image of hourglass shaped bottlebrush polymers (scale bar = 50 nm). (C) AFM image of dumbbell shaped bottlebrush polymers (scale bar = 50 nm). (D) Schematic illustration of cone-shaped tapered bottlebrush block copolymer and (E) AFM image of tapered bottlebrush block copolymer with PS side chains (scale bar = 20 nm). Reproduced with permission from references [78,80,81].

The sequential addition of macromonomer ROMP (SAM-ROMP) method is another way to prepare bottlebrush polymers with non-cylindrical morphologies. This method involves the ROMP of MMs that have varied molecular weights in sequence, with the advantage that each MM can be fully characterized and purified before use in the ROMP grafting-through step. Early work utilizing this method was carried out by Wooley and coworkers in 2012 in their synthesis of dumbbell-shaped bottlebrush polymers from an

ABA triblock bottlebrush BCP where the side chains on the first and third blocks were much longer than those on the middle block (Figure 11C).[80] More recently, this method was utilized by our group in 2017 to prepare tapered bottlebrush polymers that have a cone shape.[81] In this work, five polystyrene MMs were prepared by ATRP with M_n values ranging from 1–10 kg/mol. The SAM-ROMP of the five MMs in descending order allowed for good control over the polymerizations. The cartoon shape of the tapered bottlebrush and AFM image are shown in Figures 11D and 11E, respectively.

5.5 Linear-block-*bottlebrush BCPs*

A related class of polymers is linear-*block*-bottlebrush BCPs, as pioneered by Bowden.[55] These polymers involve the sequential ROMP of a small molecule norbornene monomer and an MM. An interesting example is the combination of linear liquid crystalline (LC) and bottlebrush PLA components as reported by Kasi and coworkers in 2020.[82] In this study, the authors explored the effects of varying the block ratios and the total molecular weight of BCPs of the structure P(Nb-CB12)-*block*-(PNb-*graft*-PLA) where Nb-CB12 = norbornene-*n*-dodecyloxycyanobiphenyl. Figure 12A shows the chemical structure and the different colors produced after processing films prepared by sequential addition of the LC monomer, where the color differences were attributed to different sizes of the photonic bandgaps as a result of self-assembly.

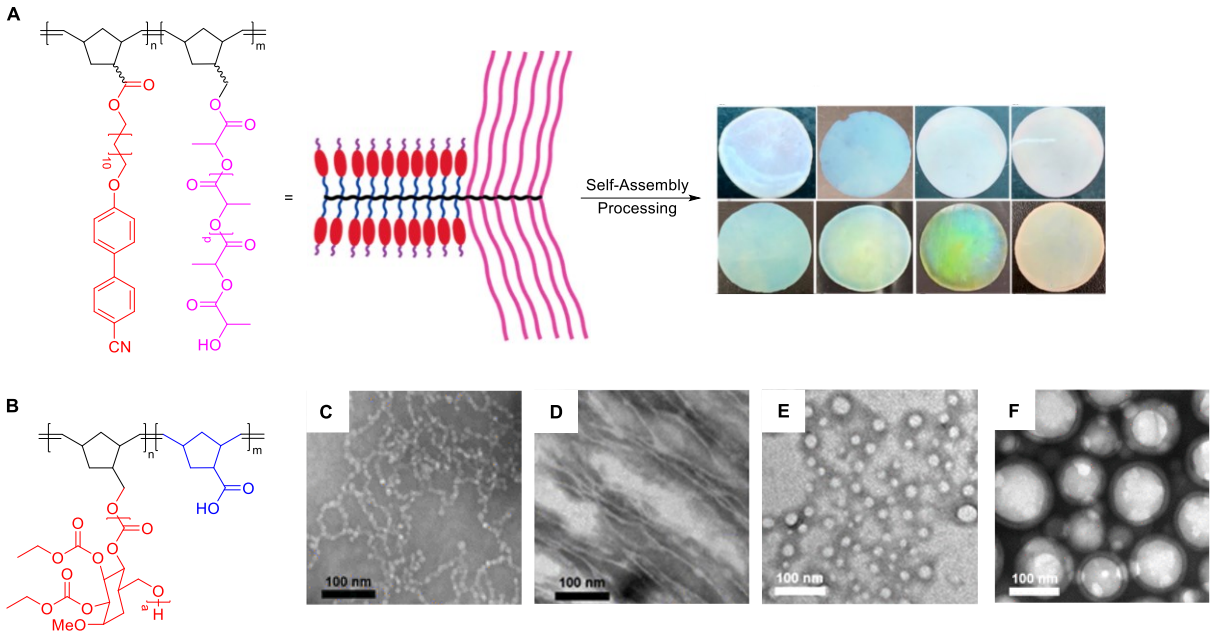

Figure 12. (A) Chemical structure of linear-*block*-bottlebrush BCP showing the self-assembly and different colors resulting from varying the block ratios. (B) Chemical structure of BCP of linear poly(acrylic acid) and bottlebrush with PCG side chains. TEM images of linear-*block*-bottlebrush BCP assemblies that form (C) elongated cylinders (D) pearl and necklace (E) spherical micelles and (F) vesicles. Adapted with permission from references [82,83].

Wooley and coworkers reported another example of linear-*block*-bottlebrush BCPs where the linear block contained norbornene carboxylic acid (Nb-COOH) and the bottlebrush block was prepared from an acetylated poly(glucose carbonate) (PGC) MM (Figure 12B).[83] The structure of the BCP, P(Nb-COOH)-*block*-(PNb-*graft*-PGC), was varied by changing N_{bb}, block ratios, and N_{sc} for the PGC bottlebrush component. In aqueous solution, the polymer assembled into different shapes including spheres, vesicles, and cylinders as shown in Figures 12C-F. The ability of the PGC component in this work to degrade into natural metabolites may enable applications of this type of structure in biomedicine, although the PNb backbone remains non-biodegradable. More broadly, with many tunable variables in linear-*block*-bottlebrush BCPs (including block ratios, N_{bb}, N_{sc}, and rigidity of the linear block and the BB block), there remains much more to explore in the self-assembly of these structures.

6. Dendronized polymers

ROMP has been used since the 1990s to synthesize dendronized polymers, a class of polymers typically made from MMs that consist of dendrons attached to polymer backbones.[84] Dendronized polymers are similar to bottlebrush polymers in that the sterically demanding dendritic unit forces an extension of the polymer backbone. However, MMs used in making dendronized polymers are monodisperse, globular structures rather than the polydisperse MMs with linear side chains used in making bottlebrush polymers. ROMP is used widely in making dendronized polymers, along with related cyclopolymerization strategies, topics that were recently reviewed by Gu.[85] Early successes in synthesizing dendronized polymers by ROMP included dendritic side chains containing up to third generation (Gen-3) dendrons.[86–89] More recent reports by Choi and coworkers have demonstrated the ability to synthesize dendronized polymers with side chain dendrons reaching up to Gen-4, Gen-5,[90] and even Gen-6.[91]

To synthesize Gen-4 and Gen-5 dendronized polymers, Choi and coworkers utilized grafting-through ROMP with MMs containing a norbornene unit linked to various amino acids. With the norbornene unit as the focal point of the dendron, the authors synthesized ester-based MMs up to Gen-2 and Gen-3[90] that underwent ROMP cleanly. However, when attempting the synthesis of a Gen-4 side chain, a temperature of 50 °C was required for the ROMP grafting-through step, which was slower and generated dendronized polymers with higher dispersity than those with only Gen-2 or Gen-3 units. This was due to the steric bulk of the dendron close to the norbornene unit, preventing efficient ROMP. The authors then examined two linkers between the norbornene unit and the dendron: an ethylene linker and a more rigid biphenyl linker (Figure 13). The ethylene linker enabled a smoother synthesis of the Gen-4 dendronized polymer with a lower dispersity than before, but a temperature of 40 °C was still required in the ROMP grafting-through step. The biphenyl linker showed the most success, and they were able to achieve a Gen-5 dendronized polymer at room temperature with low dispersity and control over the molecular weight.[90]

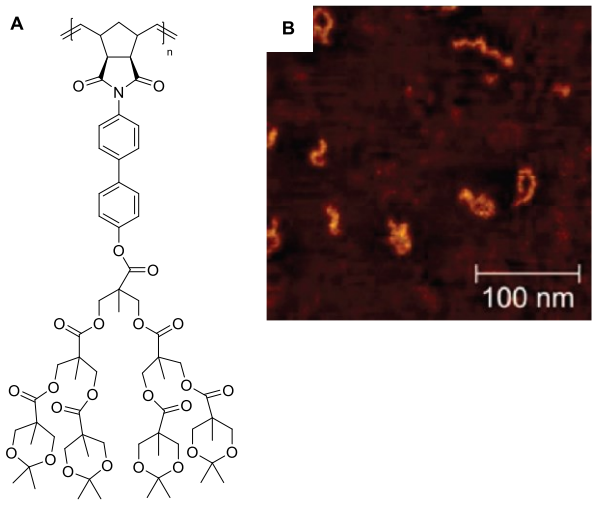

Figure 13. A) Structure of Gen-3 dendronized polymer with a biphenyl linker and B) AFM image of the Gen-3 dendronized polymer. Reproduced with permission from reference [90].

More recently, Choi and coworkers successfully synthesized a Gen-6 dendronized polymer, the largest ever achieved using the ROMP grafting-through method. Their method employed the G2 catalyst, which initiates much slower than the G3 catalyst but has similar propagation kinetics. The use of the G2 catalyst, with a monomer to initiator ratio of 100:1, enabled ROMP grafting-through at 70 °C, at which point the initiation rate was fast enough to achieve some living character. However, a maximum N_{bb} of 78 was achieved with a dispersity value of 1.45, suggesting that some catalyst death occurred or that the initiation rate remained slower than the propagation rate. The authors also synthesized the Gen-6 dendronized polymer using an Ru olefin metathesis catalyst containing a cyclic (alkyl)-(amino)carbene, which reached a higher N_{bb}. With purification by preparative SEC, they isolated a Gen-6 dendron with N_{bb} = 220 and a dispersity of 1.33.[91] Continued efforts from the Choi lab and others in making dendronized polymers, as well as dendronized BCPs and star polymers,[92–95] highlight the capabilities of the grafting-through ROMP method in polymerizing sterically bulky MMs but also reveal limitations that need to be addressed to achieve higher molecular weight and lower dispersity dendronized polymers.

7. Star polymers

A few different synthetic approaches are used to make star polymers. The core-first approach utilizes a macroinitiator as the core, and three or more arms are grown from this core. In contrast, the arm-first approach involves the synthesis of the arms followed by crosslinking to make the core. Finally, the grafting-onto approach involves the efficient coupling of the arms to a core molecule.[96] All three synthetic approaches can utilize ROMP to achieve star polymer architectures, but arm-first is most commonly used. When the arms are bottlebrush polymers, the arm-first method can be called the brush-first method, and brush-arm-star polymers (BASPs) form. BASPs, discussed below, are star polymers with bottlebrush polymer arms instead of linear arms.

Schrock and coworkers published the first few ROMP syntheses of star polymers in the early 1990s using the arm-first approach, where living PNb chains were crosslinked with a bis(norbornene species) using Mo-based ROMP catalysts.[97] The same synthetic method was later used to polymerize amphiphilic diblock arms that were then crosslinked at the end of the ROMP step to afford star BCPs, albeit with broad dispersities.[98] Although operationally straightforward, this method is typically limited to only a few arms and suffers from lack of complete control. The number of arms can be increased by increasing the ratio of crosslinking agent to the catalyst, resulting in star polymers of high MW, but excessive crosslinking can lead to gel formation.[99] Therefore, synthetic strategies involving various growth steps have been developed to maintain solubility and avoid gelation.

One interesting approach from Xia and coworkers in 2020 utilized a rigid, ladder-shaped bis(norbornene) crosslinker to form star polymers from PLA-based MMs.[100] Acidic degradation of the arms allowed for characterization of the remaining core (Figure 14), and the authors found that these rigid crosslinked cores were soluble microporous polymer nanoparticles. ROMP has also been successfully incorporated into the synthesis of miktoarm star polymers. For example, Zhang and coworkers showed in 2009 that ATRP and ROMP could be combined to make AB_2 star polymers using a core with dual functionality.[101] In this work,

they polymerized an oxanorbornene monomer that could be functionalized after ROMP with an initiator species to be used in ATRP. The subsequent polymerization introduced the two additional arms to afford the AB_2 star polymer. Miktoarm star polymers have also been made by introducing a macroterminator to a solution of MMs at the end of the ROMP step.[102]

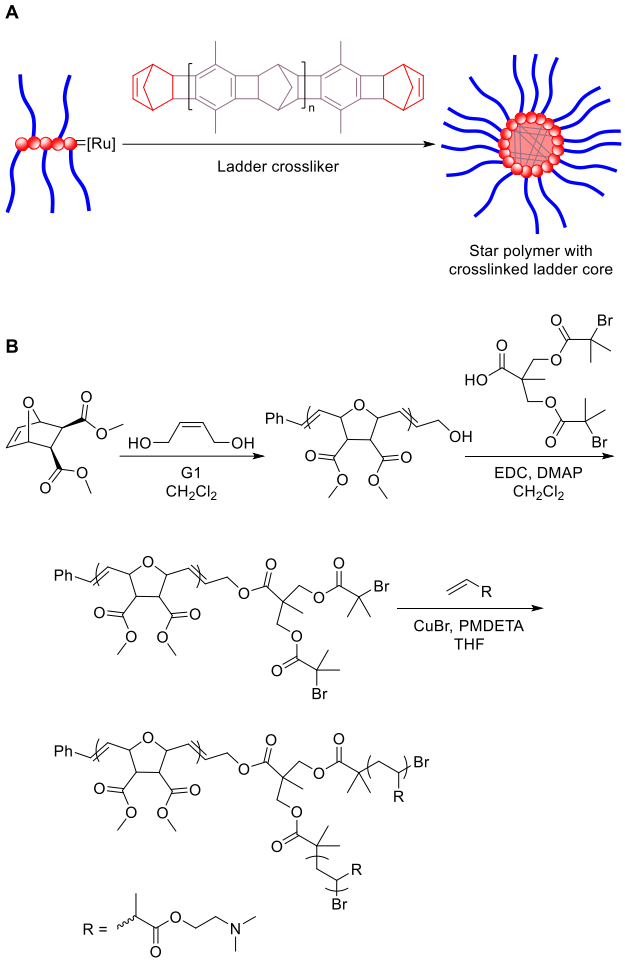

Figure 14. (A) Synthesis of star polymers with degradable arms for further characterization of the core. (B) Synthetic scheme for the synthesis of AB2 star polymers. Adapted with permission from references [100,101].

To increase the molecular weight of star polymers even further, Johnson and coworkers developed the brush-first approach to make BASPs. Their approach encourages star-star coupling only, which yields well-defined star polymers with molecular weights up to 2,300 kg/mol (Figure 15). These high MW BASPs have

been made with bottlebrush polymer arms of PEG,[103] PLA, PS,[104] and even polymers containing doxorubicin,[105,106] enabling potential application of these macromolecules in drug delivery. Another example of BASPs reported by Barnes and coworkers utilized the core-first approach.[107] In this 2020 work, which is related to a 2002 report from Verpoort and workers using dendritic cores,[108] a γ-cyclodextrin core was functionalized with 8 norbornene units that were used to grow bottlebrush polymer arms via ROMP. This method relies on equal reactivity of the initiating sites and a fast initiation using G3 catalyst to ensure a high level of control over arm number and length.

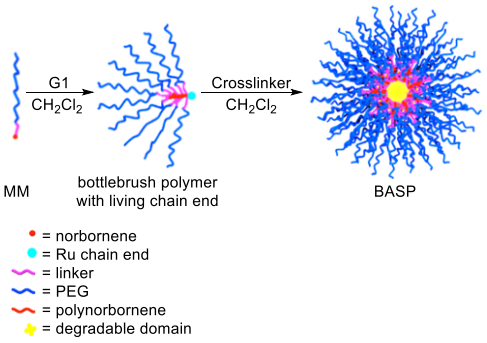

Figure 15. Synthesis of BASPs containing PEG arms and a degradable core. Reproduced with permission from reference [103].

8. Biomolecule-polymer conjugates

Star polymers synthesized using the core-first method utilize a macroinitiator, often generated *in situ* from a core with several norbornene or related groups, to create the unique star-shaped architecture. Using a similar macroinitiator approach, this method can be extended to use ROMP in the construction of biomolecule-polymer conjugates. Proteins used as biotherapeutics are often conjugated to polymers to increase the circulation lifetime of the protein, as well as to decrease protein degradation.[109] Most protein-polymer conjugates utilize the grafting-onto approach, where prepared arms such as PEG are attached to proteins, typically through surface cysteine thiols or lysine amines. ROMP enables other methods to synthesize these conjugates that may offer advantages over the grafting-onto approach. Similarly, ROMP

has been used to create DNA-polymer conjugates. We discuss a few important examples of protein-polymer and DNA-polymer conjugates below that highlight the utility of ROMP in making these complex structures. Many other types of biomolecule-polymer conjugates have also been reported that involve ROMP, including many examples where a norbornene-functionalized oligopeptide is polymerized by ROMP to make a polymer with protein-like folding, enzymatic activity, or other properties.[110–112] For the interested reader, we recommend an excellent recent review by Maynard on this topic.[113]

The grafting-to approach to create traditional biomolecule-polymer conjugates is kinetically and thermodynamically unfavorable,[114] so Isarov and Pokorski developed a grafting-from strategy using a protein-based ROMP macroinitiator in an attempt to mitigate the traditional unfavorable conditions.[115] By functionalizing lysozyme with a water-soluble Ru catalyst, they were able to grow PNb-*graft*-PEG arms from the surface of the protein (Figure 16). While this method worked, a drawback was the need for high monomer loadings due to limited access to the catalytic site on the protein, limiting control over the graft chain length.[113] In follow-up work, Pokorski and coworkers developed a grafting-to approach that attached a synthesized polymer or BCP to the protein, eliminating some of the drawbacks created in their previous work.[116]

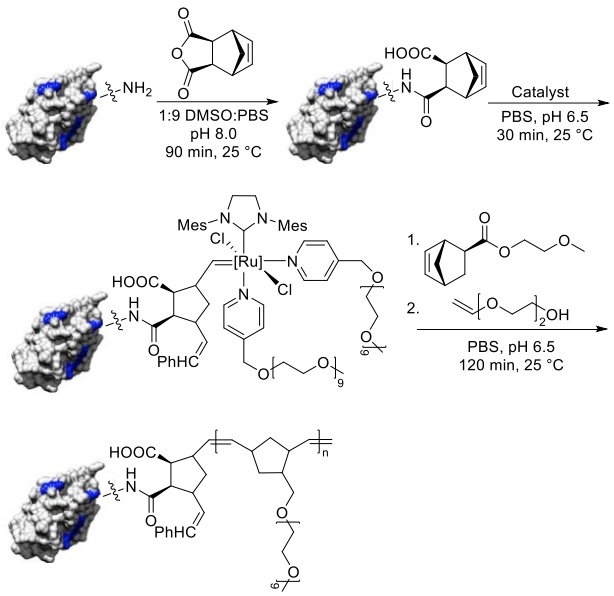

Figure 16. Synthesis of PNb-*graft*-PEG attached to a lysozyme. Adapted with permission from reference [115].

While the Pokorski group used grafting-from and grafting-to to synthesize protein-polymer conjugates, many others use the grafting-through technique to prepare biomolecule-polymer conjugates. In a 2014 example of a DNA-polymer conjugate, Zhang and coworkers used a ROMP grafting-through synthesis to make an ABA triblock copolymer of the structure (PNb-NHS)-*block*-(PNb-*graft*-PEG)-*block*-(PNb-NHS) (NHS = *N*-hydroxysuccinimidyl ester).[117] They then displaced the NHS groups with amine-modified DNA to create an ABA bottlebrush block copolymer with the outer blocks containing DNA side chains surrounding a central solubilizing PEG bottlebrush block. Interactions between the DNA units on different polymers led to a step-growth-type supramolecular polymerization in water, generating worm-like aggregates. In a 2019 study from the same group, they developed methods to directly polymerize MMs with DNA side chains using ROMP grafting-through in organic solvents by protecting the DNA. This strategy opened up synthetic access to a number of different types of complex topologies, including the direct synthesis of DNA bottlebrush BCPs of the structure (PNb-*graft*-PEG)-*block*-(PNb-DNA).[118]

9. Other ROMP Approaches to Complex Architectures

Beyond traditional methods to make homopolymers, BCPs, and multiblock copolymers, a variety of new ROMP-based methods have emerged recently that provide additional structural control, dynamics, or other advantages not available in traditional synthetic methods. Some of these methods are highlighted below.

9.1 Controlling Grafting Density and Distribution

Bottlebrush polymers have unique physical properties deriving from the densely grafted side chains, which produce a chain-extended conformation and a lack of chain entanglements.[46] While advantageous in some respects (lower viscosities at high molecular weights,[119] use as pressure-sensitive adhesives,[120] surface coatings,[121] etc.), controlling the grafting density can fundamentally change the structure-property relationship and lead to new mechanical properties,[122] physical properties,[123] and self-assembly motifs.[124] Early efforts to control grafting density utilized ATRP[125] or other RDRP copolymerizations.[126] In 2017, Grubbs and coworkers introduced a ROMP method to control grafting density and distribution with a high level of control.[127] The method relied on the copolymerization of MMs with diluent small molecule monomers with careful tuning of the reactivity ratios (Figure 17). For example, matched reactivity ratios ($r_{MM} \sim 1$, $r_{diluent} \sim 1$) afforded evenly spaced polymer grafts, while disparate reactivity ratios ($r_{MM} > 1$, $r_{diluent} < 1$ or $r_{MM} < 1$, $r_{diluent} > 1$) favored grafts on each end of the backbone chain. This method greatly expanded the tunability of bottlebrush polymer structures by enabling fine control over grafting density and distribution for a wide range of MMs and diluent monomers. A subsequent paper focusing on SAXS studies of films of these materials showed quantitatively how grafting density influences backbone stiffness.[128]

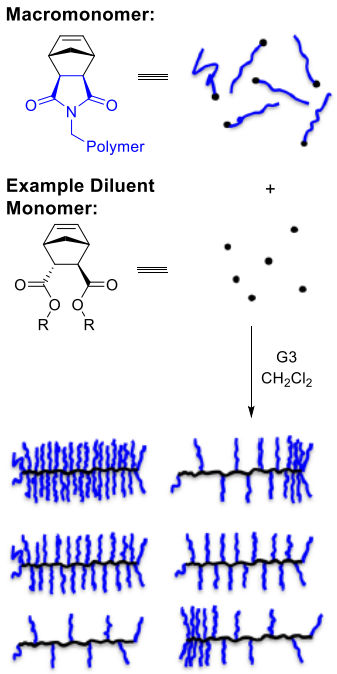

Figure 17. Schematic illustration depicting the synthesis of bottlebrush polymers with varying grafting densities made from a mixture of MMs and diluent monomers. Adapted with permission from reference [127].

9.2 Gradient BB copolymers

While bottlebrush BCPs have been discussed extensively, a unique bottlebrush copolymer includes a gradient between two different side chain polymers. In 2018, Rzayev and coworkers introduced gradient bottlebrush polymers containing PS and PLA pendant chains by taking advantage of the reactivity differences between *exo*- and *endo*-norbornene groups.[129] Typical ROMP reactions involving norbornene-functionalized monomers utilize *exo*-norbornenes because the *exo*-isomer reacts substantially faster than the *endo*-isomer (see further discussion on *endo*/*exo* norbornenes in the Practical Considerations section). When performing a homopolymerization with ROMP using a PS MM with an *exo*-norbornene, the reaction proceeded with a rate almost 30 times higher than a similar homopolymerization performed using an *endo*-functionalized PLA MM. By using predetermined feed ratios of the *endo*-Nb-PLA MM and the *exo*-Nb-PS MM, they made gradient bottlebrush polymers with differing concentrations of each side chain attached to

the PNb backbone. SAXS analysis of films of these bottlebrush copolymers revealed different morphologies depending on whether the bottlebrush polymer had a block, gradient, or statistical distribution (Figure 18).[130]

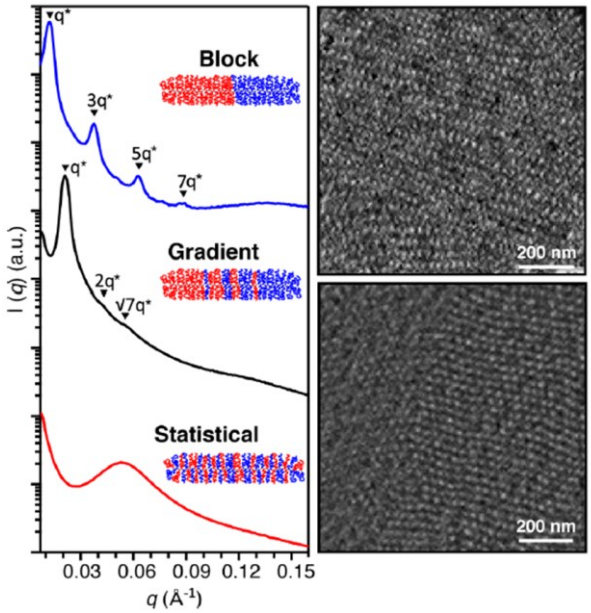

Figure 18. SAXS results (left) of block, gradient, and statistical BB copolymers and TEM images (right) of gradient bottlebrush copolymer. Reproduced with permission from reference [130].

9.3 ROMP of Polymers that Undergo Macromolecular Metamorphosis

Most polymers maintain a static topology through the end-use applications, but there is a desire to create materials with dynamic properties that change upon adjusting the environment or exposure to various stimuli.[131] Recently, Sumerlin and coworkers developed a method termed macromolecular metamorphosis for transforming a covalent polymer from one topology to a different one.[132] This work showed the transformation of amphiphilic linear block copolymers into comb polymers, hydrophobic block copolymers, and star polymers via diene displacement reactions. The residual unsaturation in polymers made by ROMP is ideal for macromolecular metamorphosis because no additional functionality is required.

Kennemur and coworkers transformed a bottlebrush polymer with a backbone made by ROMP into a linear or star polymer, highlighting the power of olefin metathesis in macromolecular metamorphosis.[133] To employ this concept, variable temperature ROMP (VT-ROMP), a method developed by the same group,[134] was used to synthesize a linear poly(cyclopentene) (PCP) with pendant bromoisobutyl groups. ATRP was then utilized in a grafting-from reaction to make bottlebrush polymers of the structure PCP-*graft*-PS or PCP-*graft*-(PS-*block*-PMMA).[135] Addition of olefin metathesis catalyst then induced end-to-end depolymerization and ring-closing metathesis, forming linear polymers with a cyclopentenyl end group.[133] This transformation was interesting because depolymerization actually led to an increase in viscosity, consistent with the lack of entanglements in bottlebrush polymers. This transformation also exposed the reactive cyclopentenyl end group, which reacted with a trithiol species in a thiol-ene reaction, transforming bottlebrush polymers into star polymers (Figure 19).

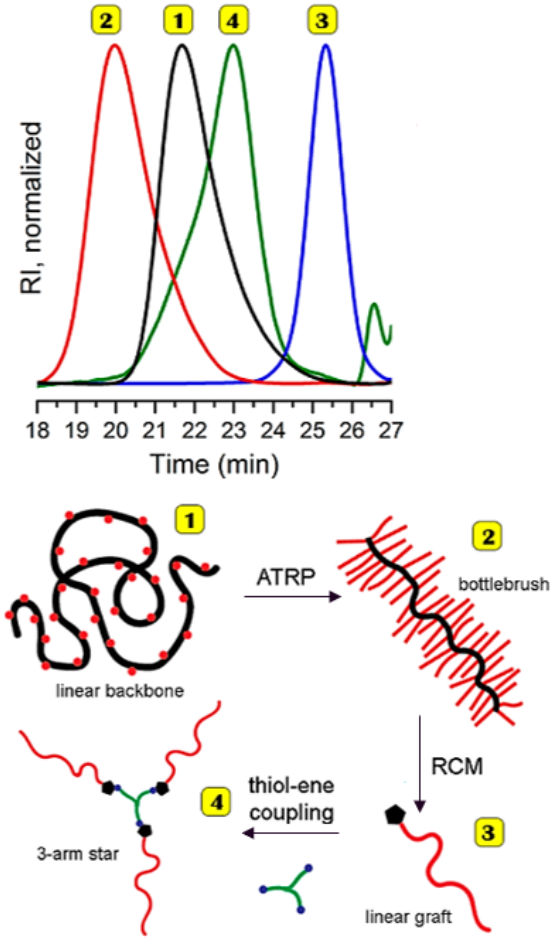

Figure 19. SEC confirmation of molecular weight changes through different stages of macromolecular metamorphosis. Adapted with permission from reference [133].

9.4 Catalytic ROMP

A drawback to performing ROMP under living conditions, regardless of the monomer, homogeneity, architecture, or morphology, is the necessity of using one catalyst equivalent for every growing polymer chain. The catalysts are expensive and present environmental and human health concerns at moderate levels, so reducing economic, environmental, and health impacts is critical. While methods involving irreversible chain transfer agents (CTAs) have been utilized to address this problem, they can lead to large

molecular weight distributions due to the intentional introduction of an irreversible terminating species.[136,137] Robotic methods utilizing linear olefin reversible CTAs have been reported, but these require specialized equipment.[138] In 2019, Kilbinger and coworkers introduced what they term "catalytic ROMP," a synthetic method that uses a reversible CTA to allow each catalyst equivalent to make more than one polymer chain.[139] Using G3 as the ruthenium catalyst, an oxanorbornene monomer, and a pyran-based reversible CTA, they were able to successfully synthesize moderately low dispersity monomers using as little as 2% of the amount of catalyst that would normally be used in non-catalytic ROMP. BCPs could also be formed this way. This method may enable new applications for materials synthesized by ROMP where contamination with residual catalyst is a concern.

10. Applications of Complex Polymer Topologies made by ROMP

ROMP has been cleverly used to synthesize several types of complex polymer topologies. In many cases, the particular topology was chosen to provide specific properties for a desired application. While applications of linear polymers prepared by ROMP have been reviewed elsewhere,[140–144] we focus here on complex topologies. Of the complex topologies discussed here, bottlebrush polymers seem to have the most potential applications due to three factors: 1) They generally do not entangle, which most linear polymers do; 2) They can exhibit shape persistence, which is also unusual in other topologies; 3) They are easily tunable, where N_{bb}, N_{sc}, graft density and distribution, and side chain chemistry can be tuned in a relatively straightforward manner. Thus, we focus in this section on emerging applications of bottlebrush polymers prepared by ROMP. For the interested reader, a few of the major potential applications with critical references include photonic crystals,[145–154] biomedicine/drug delivery,[155–165] electronic and transport materials,[166–168] elastomers[120,169–180] and nanoporous materials.[181–192] Below, we discuss specific examples of some of these applications.

Photonic crystals result when there is a periodic variation in the dielectric constant in nanostructured materials. To study this phenomenon in bottlebrush polymers, Grubbs and coworkers prepared a series of bottlebrush BCPs with side chains made of poly(isocyanate) (PI) (Figure 20A).[147] The PI side chains led to rapid self-assembly due to their rigidity. The authors tuned the photonic crystal color reflection by blending two bottlebrush BCPs with different N_{bb} values. The small and large molecular weight bottlebrush BCPs alone afforded photonic crystals with reflection bands of 360 nm and 785 nm, respectively. Blends of these two polymers with varying ratios gave photonic crystals with reflective bands that varied linearly with the blend composition between these two extremes (Figure 20B).

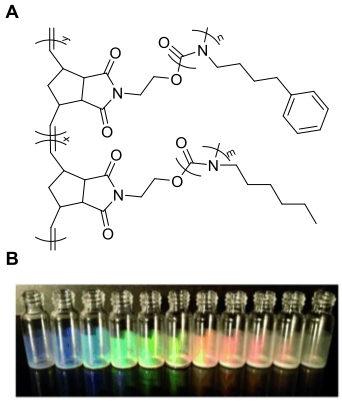

Figure 20. (A) Chemical structure of PI-based bottlebrush BCPs. (B) Photograph of brush block copolymer blends reflecting light across the visible spectrum. Adapted with permission from reference [147].

Bottlebrush homopolymers and BCPs are of interest as circulating nanocarriers due to their persistent cylindrical nanostructure, which often results in more effective drug delivery than spherical carriers.[193] Johnson and coworkers prepared water-soluble bottlebrush polymers of the general structure PNb-*graft*-PEG with the anticancer drugs doxorubicin and camptothecin covalently attached to the PNb backbone through a branch and a photodegradable linker (Figure 21A).[163] The bottlebrush BCP protected the drugs in solution, with release after UV light exposure, although the need for UV light to trigger release was noted as a downside of this system. In addition to bottlebrush polymers, doxorubicin was incorporated into the

polymeric structure of BASPs (Figure 21B), for therapeutic release in response to light, similar to the bottlebrush polymers, or pH.[105] Photoinduced degradation of the BASPs displayed similar toxicity of that of free doxorubicin towards cancerous cells. Further adaptation to these structures allowed for BASPs designed to release doxorubicin through hydrolysis rather than irradiation.[106] *In vitro* studies at physiological pH showed higher toxicity than that of free doxorubicin in cancer cells, indicating therapeutically active doxorubicin. Finally, an extension of the BASP-based nanocarriers to include three separate drugs with orthogonal release triggers showed how the molecular design of complex polymer topologies can be used to deliver chemotherapeutics with precise control over dose.[165]

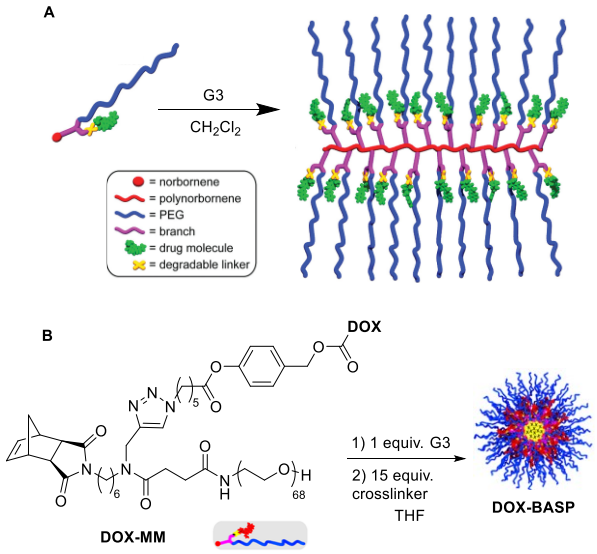

Figure 21. (A) Schematic illustration showing the components of the MM and resulting bottlebrush homopolymer with attached drug molecules. Reproduced with permission from reference [163]. (B) Chemical structure of the MM and schematic representation of the synthesis of doxorubicin-loaded BASPs. Adapted with permission from reference [106].

The absence of entanglements is a unique feature of the bottlebrush polymer topology due to their densely grafted side chains, making them super-soft elastomers upon chemical or physical crosslinking.[194] Bates and coworkers prepared elastomers based on dynamically crosslinked bottlebrush polymers of the structure PNb-*graft*-P4MCL [P4MCL = poly(4-methylcaprolactone)] crosslinked with a bislactone species at

different molecular weights and crosslinking densities.[180] Associative transesterification reactions between the P4MCL ester units and residual hydroxyl groups in the crosslinked bottlebrush polymers allowed for self-healing and dynamic stress relaxation at elevated temperatures (Figure 22). Overall, the crosslinked bottlebrush polymers reached an elongation at break of 350% and retained 85% of their toughness after two cycles of fracture and annealing.

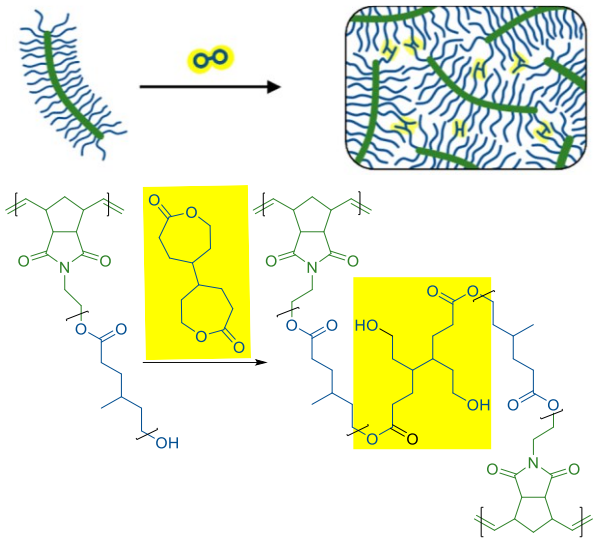

Figure 22. Reaction scheme and schematic illustration for generating dynamically crosslinked bottlebrush polymers through associative transesterification. Adapted with permission from reference [180].

The preparation of ordered porous carbon materials is of significant interest. In particular, it is difficult to create pores in the range of ~35-100 nm in diameter. Watkins and coworkers used bottlebrush BCPs of the structure (PNb-*graft*-PEG)-*block*-(PNb-*graft*-PDMS) to prepare porous carbon materials with pore sizes ranging from 16–108 nm.[192] In the bulk, the bottlebrush BCPs formed a uniform spherical morphology with the PDMS block forming the core and PEG block forming the corona. The creation of a blend of these bottlebrush BCPs with a phenol-formaldehyde resin (resol) provided a precursor to porous carbon materials after crosslinking. Finally, pyrolysis and carbonization resulted in porous carbon materials with pores that varied in size linearly with the molecular weight of the bottlebrush BCP (Figure 23).

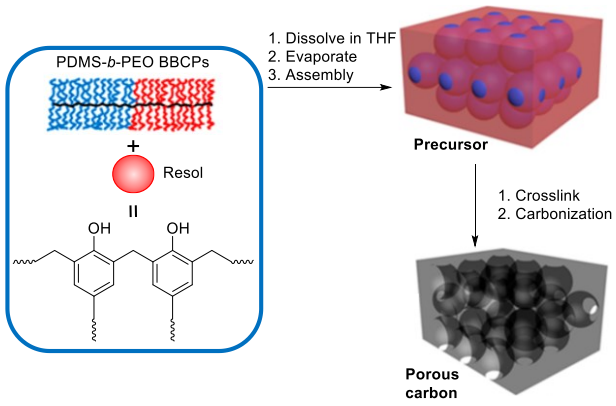

Figure 23. Schematic illustration showing the molecular structure, self-assembly, and carbonization leading to nanoporous carbon materials. Adapted with permission from reference [192].

Finally, nanoscale electronic devices have emerged as applications of bottlebrush multiblock copolymers. Hudson and coworkers recently prepared a series of multiblock bottlebrush copolymers made from ordered sequences of polyacrylate MMs using ATRP followed by ROMP grafting-through.[167] The polymers reached molecular weights exceeding 2,000 kg/mol, and the authors attributed these high molecular weights to a C11 spacer between the norbornene and the polyacrylate side chains. The bottlebrush ABC triblock copolymer imitated the design of a four-component organic light emitting diode (OLED). The three blocks included four different semiconducting components, including an electron-transport layer (ETL), an emissive layer (EML) copolymerized with another phosphorescent macromonomer that contains 8% iridium (Ir), and a hole-transport layer (HTL) (Figure 24A). This ABC bottlebrush triblock copolymer of the structure poly(Nb-*graft*-ETL)-*block*-poly(Nb-graft[EML-*co*-Ir])-*block*-poly(Nb-*graft*-HTL) formed cylindrical nanofibers (Figure 24B) without the need for crystallization, selective solvation, or supramolecular interactions. Interestingly, this nanoscale phosphorescent OLED exhibited the photophysical characteristics of each of the four organic semiconductors independently.

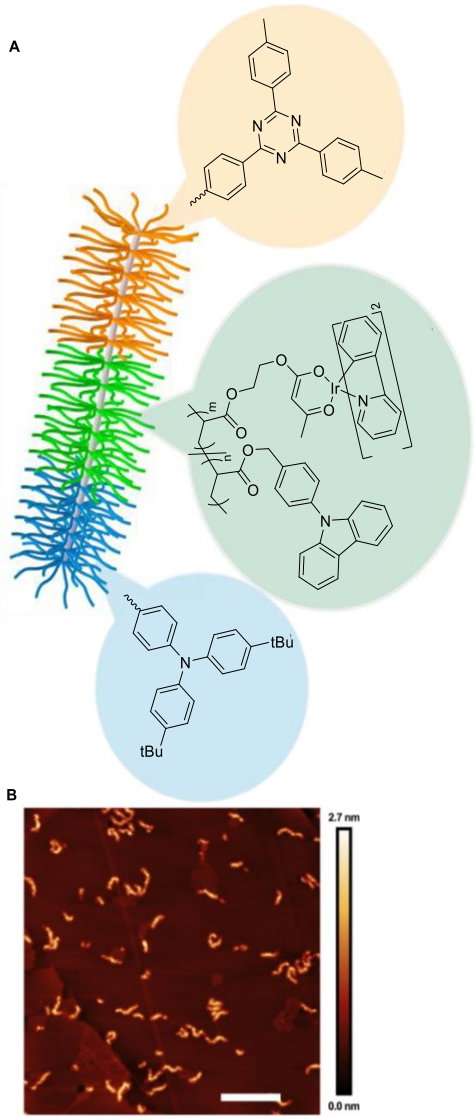

Figure 24. (A) Schematic illustration of the color-coded ABC bottlebrush triblock copolymer where ETL is orange, EML is green, and HTL is blue. (B) AFM image of bottlebrush triblock copolymer with scale bar = 200 nm. Adapted with permission from reference [167].

11. Practical Considerations

ROMP is a powerful method capable of producing several different complex polymer topologies. In many methods, ROMP works in tandem with other polymerization techniques, where ROMP is often the final step in the synthesis. ROMP is well-known for its functional group tolerance and ability to polymerize

MMs quickly, enabling the construction of complex topologies displaying a wide variety of functional groups. However, limitations remain. For example, in bottlebrush polymer synthesis, ROMP of even moderate molecular weight MMs (N_{sc} ~50) can be challenging, as can even relatively low target N_{bb} values (N_{bb} ~100), where broadening of SEC traces compared to smaller bottlebrush polymers is regularly observed. This difficulty is amplified in bottlebrush multiblock copolymer synthesis and the construction of non-centrosymmetric structures such as tapered bottlebrush polymers. Similar challenges exist in the synthesis of dendronized polymers and BASPs. Control over grafting density may appear straightforward through copolymerization of MMs and diluent (small-molecule) monomers, but careful attention must be paid to the reactivity ratios of the two monomers types.[127] Recent advances in alternating ROMP by Xia[195] and Sampson[196] may enable precise control over the spacing of side chains at intervals greater than those typically achievable in ROMP of norbornene-based MMs. Altogether, the synthesis of complex polymer topologies while controlling parameters including N_{sc}, N_{bb}, and grafting density requires highly tuned polymerizations. Figure 25 highlights some of the elements of the MM and the ROMP reaction conditions that influence the outcome of the polymerization.

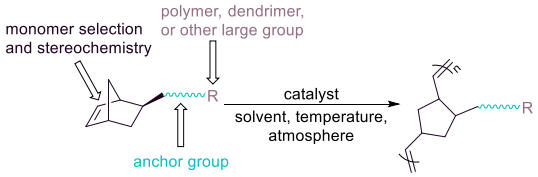

Figure 25. Schematic representation of the factors that influence the rate of ROMP.

The efficiency of ROMP relies heavily on the particular catalyst; therefore, extensive research has been done on the various catalysts as well as the invention of new catalysts to fit more specific reaction conditions. Rates of initiation and propagation dramatically influence the precision of the final polymers. The most commonly used catalysts for ROMP are the Ru-based Grubbs' catalysts. Of these, G3 catalyst (either with pyridine or bromopyridine ligands) is the most widely used catalyst, especially for norbornene species, as it has the fastest initiation and propagation rates of the common Grubbs' catalysts.[13,197,198]

However, G3 catalyst is less stable in solution than other ROMP catalysts and may not be the best option for polymerizations requiring reaction times of more than a few hours. G1 catalyst propagates slower than G3 catalyst by a factor of 10-100, but it also initiates quickly and lives longer in solution than G3 catalyst, making G1 catalyst still a widely used catalyst for ROMP. Unlike G1 catalyst and G3 catalyst, G2 catalyst and common variations of the G2 catalyst (e.g. HG2) rarely work well for polymerizations where living characteristics are needed, including molecular weight control and the capacity for chain extension, because the rate of initiation is slower than the rate of propagation.[199] In fact, in extreme scenarios where initiation is very slow compared with propagation, i.e., in latent catalysts at certain temperatures,[200] the monomer/initiator ratio plays no role in controlling molecular weight. In some cases, however, G2 catalyst can be effective for ROMP with living characteristics when monomers or MMs propagate slowly enough that control over the polymerization is maintained. In addition to the widely used Ru catalysts, Mo-based Schrock catalysts are also used in some cases due to their high activity and tacticity control,[201] although care must be taken to avoid oxygen, water, and certain functional groups.[202] Additional catalysts have been synthesized for use in more niche conditions of ROMP (e.g., aqueous ROMP), generally stemming from already published catalyst structures.

In addition to catalyst choice, investigations into optimizing the conditions of ROMP (e.g., atmosphere, temperature, solvent, concentration) have been mostly geared toward the synthesis of bottlebrush polymers. However, lessons learned in bottlebrush polymer synthesis can be applied to a variety of the architectures discussed. As mentioned, the stability of the catalyst may determine the atmosphere needed to carry out ROMP. Although many opt for the air-stable Ru catalysts, extensive research into catalysts requiring an inert atmosphere has compelled many researchers to continue using dry and air-free conditions. This is despite many examples of ROMP reactions reaching high conversion and producing well-defined polymers while open to air using Ru catalysts. At this point, we are unaware of any systematic studies comparing ROMP carried out under air to those conducted in an inert-atmosphere glovebox. Recent work by Fogg and coworkers on ring-closing metathesis revealed O_2-dependent decomposition mechanisms,[203] but whether

these would be active in ROMP is unclear because of the different propagating species (methylidene versus alkylidene). Choice of catalyst can also determine the best temperature to use for ROMP. Most of the syntheses discussed carry out ROMP at room temperature; however, a few studies suggest that elevated temperatures are preferable, mostly in the case of G2 and G1 catalysts. For example, G1 was used at 80 °C to synthesize a core-shell bottlebrush BCP.[204] In another recent example, G3 was used at temperatures up to 55°C to increase the rate of initiation for monomers with low ring strain, then the reaction mixtures were cooled in a VT-ROMP process.[134]

Solvent and (macro)monomer concentration have emerged as crucial variables regardless of the choice of catalyst for achieving well-defined polymers by ROMP. Studies have been conducted on both Schrock's and Grubbs' catalysts to determine their behavior in various organic solvents. Fontanille and coworkers investigated solvent effects on a Schrock-type catalyst, finding that cyclohexane and toluene proceeded with high rates of propagation while THF formed a complex with the Mo-based catalyst decreasing the rate of propagation by over ~4-fold.[205] In terms of Grubbs' catalysts, Sanford, Love, and Grubbs determined that the initiation rates of G1 and G2 were roughly proportional to the dielectric constant of the solvent.[11] However, Percy and coworkers measured the rate of initiation of G2 and HG-2 catalysts in nine different organic solvents and found only a slight relationship between initiation rate and solvent dielectric constant.[206] Focusing on G3, a recent study from our lab compared solvent type and purity for the synthesis of bottlebrush polymers using grafting-through ROMP studying six commonly used solvents (Figure 26). We found several key factors in selecting a solvent for a G3-catalyzed ROMP: First, purification of the solvent is unnecessary in most cases, although it was required for THF. Second, solvent influences the rate of propagation and the rate of catalyst decomposition, with EtOAc leading to a propagation rate ~2-4 times faster than the other tested solvents. Third, in terms of livingness, toluene was the best solvent in these studies due to its very low decomposition rate compared to all of the other solvents, but EtOAc and CH_2Cl_2 also show good living behavior during ROMP.[207] In terms of monomer concentration, we generally find that ROMP improves (i.e., highest achievable N_{bb} increases and dispersity decreases) with increasing initial

MM concentration, up to a point where the reaction mixture becomes highly viscous. However, others have noted no improvement in ROMP with increased (macro)monomer concentration.[91] We speculate that the optimal concentration for a ROMP reaction depends greatly on the specific system.

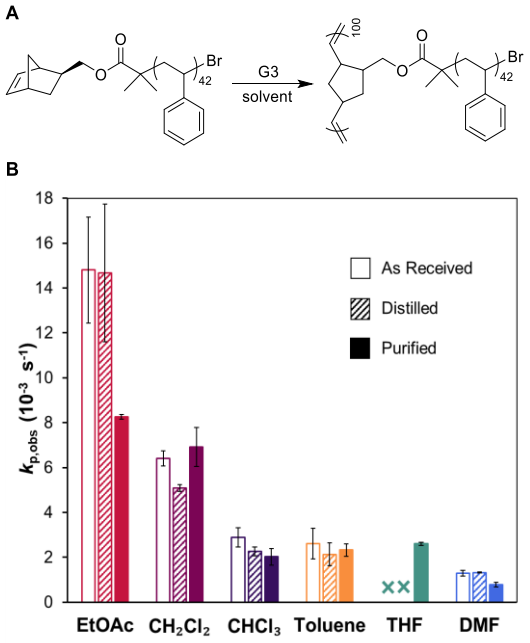

Figure 26. A) Reaction scheme of the ROMP grafting-through reaction used in the solvent studies. B) Measured first-order $k_{p,obs}$ values for this ROMP grafting through reaction in six organic solvents with differing levels of purity (as received, distilled, and purified). The $k_{p,obs}$ value for ROMP in EtOAc actually decreases with purification due to removal of an acetic acid impurity. The as received and distilled THF showed <3% conversion to BB polymer, so $k_{p,obs}$ could not be determined in these two cases. Reproduced with permission from reference [207].

Finally, the (macro)monomer structure makes a dramatic difference in the rate of propagation in ROMP and thus the "livingness" of the polymerization. Norbornenes are used widely because of their ease of synthesis and functionalization, high ring strain, and fast propagation kinetics. Oxanorbornenes are sometimes favored over norbornenes because the backbone of the resulting polymer is somewhat less hydrophobic, however, they suffer from low thermal stability due to their tendency to undergo retro-Diels-Alder reactions, generating furan.[208] Therefore, we focus here on norbornene-based monomers, where the

main factors are 1) the stereochemistry at the 5 and/or 6 positions (the two carbons opposite the carbon-carbon double bond), which can be either *endo* or *exo*, 2) the choice of anchor group, which describes the atoms connecting the norbornene unit to the 'R' group in Figure 25, where R can be a biomolecule, dendron, polymer, or other units, and 3) the size of the R group.

Substituted norbornenes are used widely in ROMP, specifically 5-substituted or 5,6-substituted, and the factor that influences the propagation rate the most is the *endo*/*exo* stereochemistry. It has been known for decades that *exo*-norbornene monomers polymerize faster than the equivalent *endo* structures by a factor of 20–100.[209,210] This phenomenon has been validated across various catalysts, solvents, and substituents, and it is largely attributed to steric effects and the fact that Lewis basic units such as esters can coordinate to the catalyst in *endo* monomers.[10,211–213] Therefore, *exo* monomers are used much more widely than *endo* monomers, despite their substantially higher cost and need for extended synthetic procedures and purifications compared with the cheaper and more widely available *endo* monomers.[214,215] However, *endo* monomers remain useful in specific scenarios, including as diluent monomers and in cases where gradient structures are targeted.[127]

Beyond the *endo*/*exo* stereochemistry, our group found in 2016 that the rate of ROMP in a series of *exo* MMs depends on the choice of anchor group, a term originally coined by Slugovc,[216] which describes the atoms connecting the norbornene unit to a functional group or polymer side chain.[217] We observed a ~5-fold difference in propagation rates between different sets of three MMs with different anchor groups, and we determined that the effect appears to be related to the HOMO energy of the (macro)monomer. The choice of anchor group dramatically affected the ultimate N_{bb} achievable for MMs with similar molecular weights, from ~140 for an imide anchor group to >800 for a specific ester anchor group. Further investigations into the mechanism of ROMP by Guironnet confirmed that the rate-determining step is the formation of the metallocyclobutane ring when using norbornene based monomers, which further highlights the importance of monomer/anchor group choice.[214]

Lastly, varying the molecular weight of the monomer, specifically referring to the N_{sc} of MMs used for the synthesis of bottlebrush polymers, affects the dispersity of the resulting polymer and the maximum conversion or maximum N_{bb} under a given set of conditions. In fact, this effect was observed by Khosravi and coworkers in 1997 in a study involving ROMP of MMs using a Schrock Mo catalyst.[218] The authors noted differences in ultimate conversion for MMs of various molecular weights and suggested that there is an N_{bb} limit that varies inversely with N_{sc}. This result is consistent with observations in our lab and others, but the N_{bb} limit appears to depend not only on N_{sc} but also on the other structural and reaction condition parameters discussed here. We attribute this effect to the ratio of propagation rate (k_p) to termination rate (k_t, i.e., catalyst decomposition rate), which Matyjaszewski has shown is a measure of "livingness".[219] In the case of ROMP, k_t appears to depend mostly on the specific catalyst and solvent, while k_p depends on these factors in addition to (macro)monomer structure. Therefore, optimization of structural features and reaction conditions in ROMP to achieve a high k_p/k_t ratio is needed to encourage high conversion for challenging (macro)monomers.

12. Challenges, Opportunities, and Future Outlook

ROMP has enabled the synthesis of a dizzying array of complex polymer topologies over the past few decades. Catalyst development in the 1990s and early 2000s directly led to these advances, with the fast initiation and slow termination (catalyst decomposition) rates of the Mo- and Ru-based catalysts providing synthetic access to multi-block polymers, star polymers, dendronized polymers, and many types of bottlebrush (co)polymers, among others. It may seem that we are only constrained by our imagination at this point, and that any envisioned structure can be synthesized. In many cases this is true, as evidenced by the array of structures and potential uses of these polymers detailed above. However, limitations remain, particularly in the synthesis of complex bottlebrush and dendronized (co)polymer topologies by ROMP grafting-through. For example, bottlebrush polymer syntheses are generally limited to relatively low N_{sc} or N_{bb} values due to the trade-off between these two elements. This limitation becomes particularly important

when high aspect ratio nanostructures (i.e., worm-shaped polymers) are desired because the globular to worm transition happens near N_{bb} ~120.[220] High N_{bb} values are also needed in many materials applications of bottlebrush polymers, such as super-soft elastomers. Dendronized polymers and BASPs also are limited to low N_{bb} values with N_{sc} values or high generation number dendrons.

Several ways can be envisioned to address these current limitations. First, improved catalyst design is a potential avenue for innovation. Olefin metathesis catalysts have typically been developed and tested with a focus on pharmaceutically relevant ring-closing metathesis reactions.[221] Rarely are they designed with ROMP in mind because most olefin metathesis catalysts can easily and quickly complete many turnovers of small, high-strain monomers such as cyclooctadiene or norbornene. In fact, G3 with two pyridine ligands, the catalyst used most widely in ROMP to make complex polymer architectures, was developed as a precursor to other catalysts, not as a catalyst by itself.[11] It was 18 months later when the bromo-pyridine version of G3 was established as a fast-initiating catalyst for ROMP.[198] These two versions of the G3 catalyst remain the standard today for ROMP with living characteristics, over 20 years after their first report. Despite the high activity of these catalysts, there seems to be room for the development of catalysts optimized for ROMP of large MMs and other sterically demanding monomers.

Second, best practices for optimizing "livingness" in ROMP mediated by existing catalysts such as G3 continue to be discovered. For example, a handful of papers address optimizing monomer type, reaction solvent, anchor group, linker length and rigidity, or reaction conditions (concentration, temperature, atmosphere) in the construction of complex topologies by ROMP. Many such best practices are detailed in the Practical Considerations sections above. However, few conclusions on optimal reaction conditions are derived from broad, systematic studies. In most cases, optimal conditions are empirically determined for a specific system, and it is unclear how such conditions might translate to other systems. Thus, there remains more to do and discover in order to synthesize larger (co)polymers with narrower dispersity values than currently accessible. In this respect, ROMP lags well behind other polymerization techniques such as ATRP, where many careful and thorough studies on ligands, solvents, initiators and other factors form a

solid foundation of understanding. This knowledge foundation is critical for especially demanding structures such as tapered bottlebrush polymers, where the catalyst is repeatedly under monomer starved conditions.

Beyond making larger structures, the lack of (bio)degradability and the potential toxicity resulting from catalyst residue has always been a concern in ROMP polymers, whether simple or complex. Polymers made by ROMP such as bottlebrush polymers and BASPs hold potential as drug delivery vehicles, but both concerns need to be addressed before any such polymers can be translated into the clinic. Fortunately, two recent discoveries may help. First, Xia and coworkers showed in 2020 that cyclic enol ethers could be polymerized by ROMP, upending the long-held belief that Fischer carbenes were metathesis inactive.[222] The resulting poly(enol ethers) are degradable under acidic conditions. This group also showed in 2021 that enol ethers such as 2,3-dihydrofuran can be copolymerized with norbornene-based monomers, including even a small MM, opening a synthetic route to degradable bottlebrush polymers.[223] Other advances in monomers with acetal linkages[25,224] and silyl ether linkages[225] also are poised to increase applications of ROMP in biomedicine. Related to these materials are ROMP polymers that can be depolymerized via olefin metathesis routes, such as those developed by Wang,[226,227] Register,[228] and Kennemur,[133,229] which may find use as materials with on-demand degradability. Second, Boydston and coworkers developed the first example of metal-free ROMP in 2015, relying on an organic photoredox mediator to conduct ROMP with radical cations as the propagating species.[230] Advances over the past few years from this group have increased the substrate scope and molecular weight control for metal-free ROMP, even providing synthetic access in some cases to polymers that are difficult to make using traditional catalysts.[231] Further development of this wholly organic form of ROMP may address concerns over residual metal toxicity.

As synthetic limitations decrease and the versatility of ROMP continues to increase, we see several application areas that are ripe for future advances in ROMP of complex topologies. Already mentioned is the use of ROMP in the construction of vehicles for drug delivery, where new innovations should eliminate long-standing problems in lack of degradability and toxicity, driving growth in this area. Another area that

we expect will see increased attention in the near future is self-assembly. Bottlebrush and dendronized BCPs assembled in the solid-state can create photonic crystals, where control over N_{sc} and N_{bb} and grafting density in both blocks in these architectures allows the researcher to tune domain spacing and color. In addition, the creation of these types of nanostructured films from polymers made by ROMP grafting-through offers a level of tunability not accessible through other polymerization routes. Solution self-assembly studies of bottlebrush BCPs and multiblock copolymers are also beginning to reveal how the many tunable variables in these complex topologies influence self-assembled morphology. We anticipate that studies on assemblies of bottlebrush and dendronized BCPs and multiblock copolymers in solution will continue to emerge, demonstrating how complex polymer topologies can enable access to nanostructured assemblies inaccessible with linear BCPs and multiblock copolymers. Finally, applications of complex nanostructures prepared by ROMP seem poised to make inroads in electronic applications, again as a result of the capacity for high levels of structural control. Further along the horizon are fundamental studies and potential applications of asymmetric or non-centrosymmetric materials prepared by ROMP. This includes tapered bottlebrush polymers, where three-dimensional nanostructured cones, hourglasses, and other shapes are difficult to attain via other routes, and ROMP provides a modular platform for innovation.

In summary, ROMP has emerged as a powerful tool over the past few decades for synthesizing complex polymer topologies. Unbound by the undesired radical-radical side reactions that limit RDRP methods and the stringent conditions and functional group restrictions imposed by anionic polymerization, ROMP in many cases provides the simplest route to star, BASP, dendronized, and bottlebrush homopolymers, BCPs, and multi-block copolymers. These complex polymer topologies are well suited to find uses as drug delivery vehicles, in nanoscale constructs, as elastomers with unusual properties, and as high-value components in devices requiring light manipulation or energy storage/conversion. Further development of the field will require innovations in catalyst and monomer design, as well as careful and systematic studies on how reaction parameters influence rates and polymer structures. Ultimately, continued efforts will

broaden the scope and size of polymers and topologies achievable by ROMP, driving fundamental studies on how polymer topology influences properties and encouraging new applications.

Acknowledgements

This work was supported by the Army Research Office (W911NF-19-1) and a joint grant between the National Science Foundation and the Binational Science Foundation (DMR-2104602). Any opinions, findings, and conclusions or recommendations expressed in this material are those of the authors and do not necessarily reflect the views of the funding agencies.

References:

(1) Jenkins, A. D.; Kratochvíl, P.; Stepto, R. F. T.; Suter, U. W. Glossary of Basic Terms in Polymer Science (IUPAC Recommendations 1996). *Pure Appl. Chem.* **1996**, *68* (12), 2287–2311. https://doi.org/10.1351/pac199668122287.

(2) Houtz, R. C.; Adkins, H. The Catalysis of Polymerization by Ozonides. II1. *J. Am. Chem. Soc.* **1933**, *55* (4), 1609–1617.

(3) Flory, P. J. The Mechanism of Vinyl Polymerizations1. *J. Am. Chem. Soc.* **1937**, *59* (2), 241–253.

(4) Alfrey, T.; Bandel, D. Paper presented at 118th *Am. Chem. Soc.* Meeting, Chicago, Sept. 4, **1950**, through Mark, H. F., *Rec. Chem. Progr.*, **1951**, *12*, 139. 1950.

(5) Battaerd, H. A. J.; Tregear, G. W. *Graft Copolymers*; John Wiley & Sons, Inc.: New York, NY, 1967.

(6) Schaefgen, J. R.; Flory, P. J. Synthesis of Multichain Polymers and Investigation of Their Viscosities [1]. *J. Am. Chem. Soc.* **1948**, *70* (8), 2709–2718. https://doi.org/10.1021/ja01188a026.

(7) Tuba, R. Synthesis of Cyclopolyolefins via Ruthenium Catalyzed Ring-Expansion Metathesis Polymerization. *Pure Appl. Chem.* **2014**, *86* (11), 1685–1693. https://doi.org/10.1515/pac-2014-0712.

(8) Nuyken, O.; Pask, S. D. Ring-Opening Polymerization—An Introductory Review. *Polymers* **2013**, *5* (2). https://doi.org/10.3390/polym5020361.

(9) Pearce, A. K.; Foster, J. C.; O'Reilly, R. K. Recent Developments in Entropy-Driven Ring-Opening Metathesis Polymerization: Mechanistic Considerations, Unique Functionality, and Sequence Control. *J. Polym. Sci. Part Polym. Chem.* **2019**, *57*, 1621–1634.

(10) Choi, T.-L.; Grubbs, R. H. Controlled Living Ring-Opening-Metathesis Polymerization by a Fast-Initiating Ruthenium Catalyst. *Angew. Chem. Int. Ed.* **2003**, *42* (15), 1743–1746. https://doi.org/10.1002/anie.200250632.

(11) Sanford, M. S.; Love, J. A.; Grubbs, R. H. Mechanism and Activity of Ruthenium Olefin Metathesis Catalysts. *J. Am. Chem. Soc.* **2001**, *123* (27), 6543–6554. https://doi.org/10.1021/ja010624k.

(12) AU - Liu, J.; AU - Gao, A. X.; AU - Johnson, J. A. Particles without a Box: Brush-First Synthesis of Photodegradable PEG Star Polymers under Ambient Conditions. *J. Vis. Exp.* **2013**, No. 80, e50874. https://doi.org/10.3791/50874.

(13) Love, J. A.; Morgan, J. P.; Trnka, T. M.; Grubbs, R. H. A Practical and Highly Active Ruthenium-Based Catalyst That Effects the Cross Metathesis of Acrylonitrile. *Angew. Chem. Int. Ed.* **2002**, *41* (21), 4035–4037. https://doi.org/10.1002/1521-3773(20021104)41:21<4035::AID-ANIE4035>3.0.CO;2-I.

(14) Bielawski, C. W.; Grubbs, R. H. Highly Efficient Ring-Opening Metathesis Polymerization (ROMP) Using New Ruthenium Catalysts Containing N-Heterocyclic Carbene Ligands. *Angew. Chem. Int. Ed. 39*, 2903–2904.

(15) Herz, K.; Elser, I.; Buchmeiser, M. R. Ring-Opening Metathesis Polymerization: Mechanisms https://onlinelibrary.wiley.com/doi/abs/10.1002/9783527815562.mme0001 (accessed 2022 -04 -19).

(16) Mankowich, A. M. Micellar Molecular Weights of Selected Surface Active Agents. *J. Phys. Chem.* **1954**, *58* (11), 1027–1030. https://doi.org/10.1021/j150521a022.

(17) Chen, Y.; Abdellatif, M. M.; Nomura, K. Olefin Metathesis Polymerization: Some Recent Developments in the Precise Polymerizations for Synthesis of Advanced Materials (by ROMP, ADMET). *Tetrahedron* **2018**, *74* (6), 619–643. https://doi.org/10.1016/j.tet.2017.12.041.

(18) Risse, W.; Grubbs, R. H. A Novel Route to Block Copolymers by Changing the Mechanism from Living Ring-Opening Metathesis Polymerization of Cyclic Olefins to Aldol Condensation Polymerization of Silyl Vinyl Ethers. *Macromolecules* **1989**, *22* (4), 1558–1562. https://doi.org/10.1021/ma00194a009.

(19) Bishop, J. P.; Register, R. A. Thermoplastic Elastomers with Composite Crystalline−Glassy Hard Domains and Single-Phase Melts. *Macromolecules* **2010**, *43* (11), 4954–4960. https://doi.org/10.1021/ma100314z.

(20) Komanduri, V.; Kumar, D. R.; Tate, D. J.; Marcial-Hernandez, R.; Lidster, B. J.; Turner, M. L. Bidirectional ROMP of Paracylophane-1,9-Dienes to Tri- and Penta-Block *p* -Phenylenevinylene Copolymers. *Polym. Chem.* **2019**, *10* (25), 3497–3502. https://doi.org/10.1039/C9PY00147F.

(21) Lang, C.; Kumar, M.; Hickey, R. J. Influence of Block Sequence on the Colloidal Self-Assembly of Poly(Norbornene)- *Block* -Poly(Ethylene Oxide) Amphiphilic Block Polymers Using Rapid Injection Processing. *Polym. Chem.* **2020**, *11* (2), 375–384. https://doi.org/10.1039/C9PY00954J.

(22) Mandal, A.; Mandal, I.; Kilbinger, A. F. M. Pulsed-Addition ROMP: Catalytic Syntheses of Heterotelechelic Polymers via Regioselective Chain Transfer Agents. *ACS Macro Lett.* **2022**, *11* (4), 491–497. https://doi.org/10.1021/acsmacrolett.2c00094.

(23) Varlas, S.; Lawrenson, S. B.; Arkinstall, L. A.; O'Reilly, R. K.; Foster, J. C. Self-Assembled Nanostructures from Amphiphilic Block Copolymers Prepared via Ring-Opening Metathesis

Polymerization (ROMP). *Prog. Polym. Sci.* **2020**, *107*, 101278. https://doi.org/10.1016/j.progpolymsci.2020.101278.

(24) Hilf, S.; Kilbinger, A. F. M. Sacrificial Synthesis of Hydroxy-Telechelic Metathesis Polymers via Multiblock-Copolymers. *Macromolecules* **2009**, *42* (4), 1099–1106. https://doi.org/10.1021/ma802440k.

(25) Hilf, S.; Berger-Nicoletti, E.; Grubbs, R. H.; Kilbinger, A. F. M. Monofunctional Metathesis Polymers via Sacrificial Diblock Copolymers. *Angew. Chem. Int. Ed.* **2006**, *45* (47), 8045–8048. https://doi.org/10.1002/anie.200602323.

(26) Rahman, M. A.; Lokupitiya, H. N.; Ganewatta, M. S.; Yuan, L.; Stefik, M.; Tang, C. Designing Block Copolymer Architectures toward Tough Bioplastics from Natural Rosin. *Macromolecules* **2017**, *50* (5), 2069–2077. https://doi.org/10.1021/acs.macromol.7b00001.

(27) Miyamoto, Y.; Fujiki, M.; Nomura, K. Synthesis of Homopolymers and Multiblock Copolymers by the Living Ring-Opening Metathesis Polymerization of Norbornenes Containing Acetyl-Protected Carbohydrates with Well-Defined Ruthenium and Molybdenum Initiators. *J. Polym. Sci. Part Polym. Chem.* **2004**, *42* (17), 4248–4265. https://doi.org/10.1002/pola.20286.

(28) Gu, H.; Ciganda, R.; Castel, P.; Ruiz, J.; Astruc, D. Living ROMP Syntheses and Redox Properties of Triblock Metallocopolymer Redox Cascades. *Macromolecules* **2016**, *49* (13), 4763–4773. https://doi.org/10.1021/acs.macromol.6b01046.

(29) Gu, H.; Ciganda, R.; Castel, P.; Moya, S.; Hernandez, R.; Ruiz, J.; Astruc, D. Tetrablock Metallopolymer Electrochromes. *Angew. Chem. Int. Ed.* **2018**, *57* (8), 2204–2208. https://doi.org/10.1002/anie.201712945.

(30) Canning, S. L.; Smith, G. N.; Armes, S. P. A Critical Appraisal of RAFT-Mediated Polymerization-Induced Self-Assembly. *Macromolecules* **2016**, *49* (6), 1985–2001. https://doi.org/10.1021/acs.macromol.5b02602.

(31) Keddie, D. J. A Guide to the Synthesis of Block Copolymers Using Reversible-Addition Fragmentation Chain Transfer (RAFT) Polymerization. *Chem Soc Rev* **2014**, *43* (2), 496–505. https://doi.org/10.1039/C3CS60290G.

(32) Figg, C. A.; Carmean, R. N.; Bentz, K. C.; Mukherjee, S.; Savin, D. A.; Sumerlin, B. S. Tuning Hydrophobicity To Program Block Copolymer Assemblies from the Inside Out. *Macromolecules* **2017**, *50* (3), 935–943. https://doi.org/10.1021/acs.macromol.6b02754.

(33) Li, Y.; Armes, S. P. RAFT Synthesis of Sterically Stabilized Methacrylic Nanolatexes and Vesicles by Aqueous Dispersion Polymerization. *Angew. Chem. Int. Ed.* **2010**, *49* (24), 4042–4046. https://doi.org/10.1002/anie.201001461.

(34) Wright, D. B.; Touve, M. A.; Adamiak, L.; Gianneschi, N. C. ROMPISA: Ring-Opening Metathesis Polymerization-Induced Self-Assembly. *ACS Macro Lett.* **2017**, *6* (9), 925–929. https://doi.org/10.1021/acsmacrolett.7b00408.

(35) Varlas, S.; Foster, J. C.; O'Reilly, R. K. Ring-Opening Metathesis Polymerization-Induced Self-Assembly (ROMPISA). *Chem. Commun.* **2019**, *55* (62), 9066–9071. https://doi.org/10.1039/C9CC04445K.

(36) Zhang, L.; Song, C.; Yu, J.; Yang, D.; Xie, M. One-Pot Synthesis of Polymeric Nanoparticle by Ring-Opening Metathesis Polymerization. *J. Polym. Sci. Part Polym. Chem.* **2010**, *48* (22), 5231–5238. https://doi.org/10.1002/pola.24323.

(37) Yoon, K.-Y.; Lee, I.-H.; Kim, K. O.; Jang, J.; Lee, E.; Choi, T.-L. One-Pot in Situ Fabrication of Stable Nanocaterpillars Directly from Polyacetylene Diblock Copolymers Synthesized by Mild Ring-Opening Metathesis Polymerization. *J. Am. Chem. Soc.* **2012**, *134* (35), 14291–14294. https://doi.org/10.1021/ja305150c.

(38) Wright, D. B.; Thompson, M. P.; Touve, M. A.; Carlini, A. S.; Gianneschi, N. C. Enzyme-Responsive Polymer Nanoparticles via Ring-Opening Metathesis Polymerization-Induced Self-Assembly. *Macromol. Rapid Commun.* **2019**, *40* (2), 1800467. https://doi.org/10.1002/marc.201800467.

(39) Wright, D. B.; Proetto, M. T.; Touve, M. A.; Gianneschi, N. C. Ring-Opening Metathesis Polymerization-Induced Self-Assembly (ROMPISA) of a Cisplatin Analogue for High Drug-Loaded Nanoparticles. *Polym. Chem.* **2019**, *10* (23), 2996–3000. https://doi.org/10.1039/C8PY01539B.

(40) Foster, J. C.; Varlas, S.; Blackman, L. D.; Arkinstall, L. A.; O'Reilly, R. K. Ring-Opening Metathesis Polymerization in Aqueous Media Using a Macroinitiator Approach. *Angew. Chem. Int. Ed.* **2018**, *57* (33), 10672–10676. https://doi.org/10.1002/anie.201806719.

(41) Foster, J. C.; Grocott, M. C.; Arkinstall, L. A.; Varlas, S.; Redding, M. J.; Grayson, S. M.; O'Reilly, R. K. It Is Better with Salt: Aqueous Ring-Opening Metathesis Polymerization at Neutral PH. *J. Am. Chem. Soc.* **2020**, *142* (32), 13878–13885. https://doi.org/10.1021/jacs.0c05499.

(42) Wintermantel, M.; Gerle, M.; Fischer, K.; Schmidt, M.; Wataoka, I.; Urakawa, H.; Kajiwara, K.; Tsukahara, Y. Molecular Bottlebrushes †. *Macromolecules* **1996**, *29* (3), 978–983. https://doi.org/10.1021/ma950227s.

(43) Li, Z.; Tang, M.; Liang, S.; Zhang, M.; Biesold, G. M.; He, Y.; Hao, S.-M.; Choi, W.; Liu, Y.; Peng, J.; Lin, Z. Bottlebrush Polymers: From Controlled Synthesis, Self-Assembly, Properties to Applications. *Prog. Polym. Sci.* **2021**, *116*, 101387. https://doi.org/10.1016/j.progpolymsci.2021.101387.

(44) Verduzco, R.; Li, X.; Pesek, S. L.; Stein, G. E. Structure, Function, Self-Assembly, and Applications of Bottlebrush Copolymers. *Chem. Soc. Rev.* **2015**, *44* (8), 2405–2420. https://doi.org/10.1039/C4CS00329B.

(45) Desimone, J. M.; Hellstern, A. M.; Siochi, E. J.; Smith, S. D.; Ward, T. C.; McGrath, J. E.; Gallagher, P. M.; Krukonis, V. J. Homogeneous and Multiphase Poly(Methyl Methacrylate) Graft Polymers via the Macromonomer Method. *Makromol. Chem. Macromol. Symp.* **1990**, *32* (1), 21–45. https://doi.org/10.1002/masy.19900320105.

(46) Sheiko, S. S.; Sumerlin, B. S.; Matyjaszewski, K. Cylindrical Molecular Brushes: Synthesis, Characterization, and Properties. *Prog. Polym. Sci.* **2008**, *33* (7), 759–785. https://doi.org/10.1016/j.progpolymsci.2008.05.001.

(47) Milner S. T. Polymer Brushes. *Science* **1991**, *251* (4996), 905–914. https://doi.org/10.1126/science.251.4996.905.

(48) Foster, J. C.; Varlas, S.; Couturaud, B.; Coe, Z.; O'Reilly, R. K. Getting into Shape: Reflections on a New Generation of Cylindrical Nanostructures' Self-Assembly Using Polymer Building Blocks. *J. Am. Chem. Soc.* **2019**, *141* (7), 2742–2753. https://doi.org/10.1021/jacs.8b08648.

(49) Foster, J. C.; Radzinski, S. C.; Matson, J. B. Graft Polymer Synthesis by RAFT Transfer-To. *J. Polym. Sci. Part Polym. Chem.* **2017**, *55* (18), 2865–2876. https://doi.org/10.1002/pola.28621.

(50) Jha, S.; Dutta, S.; Bowden, N. B. Synthesis of Ultralarge Molecular Weight Bottlebrush Polymers Using Grubbs' Catalysts. *Macromolecules* **2004**, *37* (12), 4365–4374. https://doi.org/10.1021/ma049647k.

(51) Xia, Y.; Kornfield, J. A.; Grubbs, R. H. Efficient Synthesis of Narrowly Dispersed Brush Polymers via Living Ring-Opening Metathesis Polymerization of Macromonomers. *Macromolecules* **2009**, *42* (11), 3761–3766. https://doi.org/10.1021/ma900280c.

(52) Cho, H. Y.; Krys, P.; Szcześniak, K.; Schroeder, H.; Park, S.; Jurga, S.; Buback, M.; Matyjaszewski, K. Synthesis of Poly(OEOMA) Using Macromonomers via "Grafting-Through" ATRP. *Macromolecules* **2015**, *48* (18), 6385–6395. https://doi.org/10.1021/acs.macromol.5b01592.

(53) Teo, Y. C.; Xia, Y. Importance of Macromonomer Quality in the Ring-Opening Metathesis Polymerization of Macromonomers. *Macromolecules* **2015**, *48* (16), 5656–5662. https://doi.org/10.1021/acs.macromol.5b01176.

(54) Jha, S.; Dutta, S.; Bowden, N. B. Synthesis of Ultralarge Molecular Weight Bottlebrush Polymers Using Grubbs' Catalysts. *Macromolecules* **2004**, *37* (12), 4365–4374. https://doi.org/10.1021/ma049647k.

(55) Runge, M. B.; Lipscomb, C. E.; Ditzler, L. R.; Mahanthappa, M. K.; Tivanski, A. V.; Bowden, N. B. Investigation of the Assembly of Comb Block Copolymers in the Solid State. *Macromolecules* **2008**, *41* (20), 7687–7694. https://doi.org/10.1021/ma8009323.

(56) Cheng, C.; Khoshdel, E.; Wooley, K. L. ATRP from a Norbornenyl-Functionalized Initiator: Balancing of Complementary Reactivity for the Preparation of α-Norbornenyl Macromonomers/ω-Haloalkyl Macroinitiators. *Macromolecules* **2005**, *38* (23), 9455–9465. https://doi.org/10.1021/ma0515984.

(57) Radzinski, S. C.; Foster, J. C.; Matson, J. B. Synthesis of Bottlebrush Polymers via Transfer-to and Grafting-through Approaches Using a RAFT Chain Transfer Agent with a ROMP-Active Z-Group. *Polym. Chem.* **2015**, *6* (31), 5643–5652. https://doi.org/10.1039/C4PY01567C.

(58) Patton, D. L.; Advincula, R. C. A Versatile Synthetic Route to Macromonomers via RAFT Polymerization. *Macromolecules* **2006**, *39* (25), 8674–8683. https://doi.org/10.1021/ma061382h.

(59) Li, Z.; Zhang, K.; Ma, J.; Cheng, C.; Wooley, K. L. Facile Syntheses of Cylindrical Molecular Brushes by a Sequential RAFT and ROMP "grafting-through" Methodology. **2010**, 10.

(60) Li, X.; ShamsiJazeyi, H.; Pesek, S. L.; Agrawal, A.; Hammouda, B.; Verduzco, R. Thermoresponsive PNIPAAM Bottlebrush Polymers with Tailored Side-Chain Length and End-Group Structure. *Soft Matter* **2014**, *10* (12), 2008. https://doi.org/10.1039/c3sm52614c.

(61) Naguib, M.; Nixon, K. L.; Keddie, D. J. Effect of Copolymerization of the (Oxa)Norbornene End-Group of RAFT-Prepared Macromonomers on Bottlebrush Copolymer Synthesis via ROMP. *Polym. Chem.* **2022**.

(62) Feast, W. J.; Gibson, V. C.; Johnson, A. F.; Khosravi, E.; Mohsin, M. A. Tailored Copolymers via Coupled Anionic and Ring Opening Metathesis Polymerization. Synthesis and Polymerization of Bicyclo[2.2.1]Hept-5-Ene-2,3-Trans-Bis(Polystyrylcarboxylate)s. *Polymer* **1994**, *35* (16), 3542–3548. https://doi.org/10.1016/0032-3861(94)90921-0.

(63) Zhang, H.; Zhang, Z.; Gnanou, Y.; Hadjichristidis, N. Well-Defined Polyethylene-Based Random, Block, and Bilayered Molecular Cobrushes. *Macromolecules* **2015**, *48* (11), 3556–3562. https://doi.org/10.1021/acs.macromol.5b00713.

(64) Lexer, C.; Saf, R.; Slugovc, C. Acrylates as Termination Reagent for the Preparation of Semi-Telechelic Polymers Made by Ring Opening Metathesis Polymerization. *J. Polym. Sci. Part Polym. Chem.* **2009**, *47* (1), 299–305. https://doi.org/10.1002/pola.23137.

(65) Choi, J.; Kim, H.; Do, T.; Moon, J.; Choe, Y.; Kim, J. G.; Bang, J. Influence of Residual Impurities on Ring-Opening Metathesis Polymerization after Copper(I)-Catalyzed Alkyne-Azide Cycloaddition Click Reaction. *J. Polym. Sci. Part Polym. Chem.* **2019**, *57* (6), 726–737. https://doi.org/10.1002/pola.29317.

(66) Lu, H.; Wang, J.; Lin, Y.; Cheng, J. One-Pot Synthesis of Brush-Like Polymers via Integrated Ring-Opening Metathesis Polymerization and Polymerization of Amino Acid *N* -Carboxyanhydrides. *J. Am. Chem. Soc.* **2009**, *131* (38), 13582–13583. https://doi.org/10.1021/ja903425x.

(67) Li, A.; Ma, J.; Sun, G.; Li, Z.; Cho, S.; Clark, C.; Wooley, K. L. One-Pot, Facile Synthesis of Well-Defined Molecular Brush Copolymers by a Tandem RAFT and ROMP, "Grafting-through" Strategy. *J. Polym. Sci. Part Polym. Chem.* **2012**, *50* (9), 1681–1688. https://doi.org/10.1002/pola.25954.

(68) Chatterjee, A. K.; Choi, T.-L.; Sanders, D. P.; Grubbs, R. H. A General Model for Selectivity in Olefin Cross Metathesis. *J. Am. Chem. Soc.* **2003**, *125* (37), 11360–11370. https://doi.org/10.1021/ja0214882.

(69) Radzinski, S. C.; Foster, J. C.; Matson, J. B. Preparation of Bottlebrush Polymers via a One-Pot Ring-Opening Polymerization (ROP) and Ring-Opening Metathesis Polymerization (ROMP) Grafting-Through Strategy. *Macromol. Rapid Commun.* **2016**, *37* (7), 616–621. https://doi.org/10.1002/marc.201500672.

(70) Kluthe, K. E. I.; Wagner, M.; Klapper, M. Simultaneous Bottlebrush Polymerization. *Macromolecules* **2021**, *54* (3), 1465–1477. https://doi.org/10.1021/acs.macromol.0c01724.

(71) Runge, M. B.; Bowden, N. B. Synthesis of High Molecular Weight Comb Block Copolymers and Their Assembly into Ordered Morphologies in the Solid State. *J. Am. Chem. Soc.* **2007**, *129* (34), 10551–10560. https://doi.org/10.1021/ja072929q.

(72) Xia, Y.; Olsen, B. D.; Kornfield, J. A.; Grubbs, R. H. Efficient Synthesis of Narrowly Dispersed Brush Copolymers and Study of Their Assemblies: The Importance of Side Chain Arrangement. *J. Am. Chem. Soc.* **2009**, *131* (51), 18525–18532. https://doi.org/10.1021/ja908379q.

(73) Li, Z.; Ma, J.; Cheng, C.; Zhang, K.; Wooley, K. L. Synthesis of Hetero-Grafted Amphiphilic Diblock Molecular Brushes and Their Self-Assembly in Aqueous Medium. *Macromolecules* **2010**, *43* (3), 1182–1184. https://doi.org/10.1021/ma902513n.

(74) Su, L.; Heo, G. S.; Lin, Y.-N.; Dong, M.; Zhang, S.; Chen, Y.; Sun, G.; Wooley, K. L. Syntheses of Triblock Bottlebrush Polymers through Sequential ROMPs: Expanding the Functionalities of Molecular Brushes. *J. Polym. Sci. Part Polym. Chem.* **2017**, *55* (18), 2966–2970. https://doi.org/10.1002/pola.28647.

(75) Onbulak, S.; Rzayev, J. Synthesis and One-Dimensional Assembly of Cylindrical Polymer Nanoparticles Prepared from Tricomponent Bottlebrush Copolymers. *J. Polym. Sci. Part Polym. Chem.* **2017**, *55* (23), 3868–3874. https://doi.org/10.1002/pola.28771.

(76) Nguyen, H. V.-T.; Gallagher, N. M.; Vohidov, F.; Jiang, Y.; Kawamoto, K.; Zhang, H.; Park, J. V.; Huang, Z.; Ottaviani, M. F.; Rajca, A.; Johnson, J. A. Scalable Synthesis of Multivalent Macromonomers for ROMP. *ACS Macro Lett.* **2018**, *7* (4), 472–476. https://doi.org/10.1021/acsmacrolett.8b00201.

(77) Nam, J.; Kim, Y.; Kim, J. G.; Seo, M. Self-Assembly of Monolayer Vesicles via Backbone-Shiftable Synthesis of Janus Core–Shell Bottlebrush Polymer. *Macromolecules* **2019**, *52* (24), 9484–9494. https://doi.org/10.1021/acs.macromol.9b01429.

(78) Walsh, D. J.; Dutta, S.; Sing, C. E.; Guironnet, D. Engineering of Molecular Geometry in Bottlebrush Polymers. *Macromolecules* **2019**, *52* (13), 4847–4857. https://doi.org/10.1021/acs.macromol.9b00845.

(79) Walsh, D. J.; Guironnet, D. Macromolecules with Programmable Shape, Size, and Chemistry. *Proc. Natl. Acad. Sci.* **2019**, *116* (5), 1538. https://doi.org/10.1073/pnas.1817745116.

(80) Li, A.; Li, Z.; Zhang, S.; Sun, G.; Policarpio, D. M.; Wooley, K. L. Synthesis and Direct Visualization of Dumbbell-Shaped Molecular Brushes. *ACS Macro Lett.* **2012**, *1* (1), 241–245. https://doi.org/10.1021/mz200184f.

(81) Radzinski, S. C.; Foster, J. C.; Scannelli, S. J.; Weaver, J. R.; Arrington, K. J.; Matson, J. B. Tapered Bottlebrush Polymers: Cone-Shaped Nanostructures by Sequential Addition of Macromonomers. *ACS Macro Lett.* **2017**, *6* (10), 1175–1179. https://doi.org/10.1021/acsmacrolett.7b00724.

(82) Ndaya, D.; Bosire, R.; Kasi, R. M. Spherical Photonic Nanostructures from High Molecular Weight Liquid Crystalline Brushlike Block Copolymers. *ACS Appl. Polym. Mater.* **2020**, *2* (12), 5511–5520. https://doi.org/10.1021/acsapm.0c00856.

(83) Dong, M.; Wessels, M. G.; Lee, J. Y.; Su, L.; Wang, H.; Letteri, R. A.; Song, Y.; Lin, Y.-N.; Chen, Y.; Li, R.; Pochan, D. J.; Jayaraman, A.; Wooley, K. L. Experiments and Simulations of Complex Sugar-Based Coil−Brush Block Polymer Nanoassemblies in Aqueous Solution. *ACS Nano* **2019**, *13* (5), 5147–5162. https://doi.org/10.1021/acsnano.8b08811.

(84) Schlüter, A. D.; Rabe, J. P. Dendronized Polymers: Synthesis, Characterization, Assembly at Interfaces, and Manipulation. *Angew. Chem. Int. Ed.* **2000**, *39* (5), 864–883. https://doi.org/10.1002/(SICI)1521-3773(20000303)39:5<864::AID-ANIE864>3.0.CO;2-E.

(85) Liu, X.; Liu, F.; Liu, W.; Gu, H. ROMP and MCP as Versatile and Forceful Tools to Fabricate Dendronized Polymers for Functional Applications. *Polym. Rev.* **2021**, *61* (1), 1–53. https://doi.org/10.1080/15583724.2020.1723022.

(86) Percec, V.; Schlueter, D.; Ronda, J. C.; Johansson, G.; Ungar, G.; Zhou, J. P. Tubular Architectures from Polymers with Tapered Side Groups. Assembly of Side Groups *via* a Rigid Helical Chain Conformation and Flexible Helical Chain Conformation Induced *via* Assembly of Side Groups. *Macromolecules* **1996**, *29* (5), 1464–1472. https://doi.org/10.1021/ma951244k.

(87) Percec, V.; Holerca, M. N. Detecting the Shape Change of Complex Macromolecules during Their Synthesis with the Aid of Kinetics. A New Lesson from Biology. *Biomacromolecules* **2000**, *1* (1), 6–16. https://doi.org/10.1021/bm005507g.

(88) Rajarm, S.; Choi, T.-L.; Rolandi, M.; Frechet, J. M. J. Synthesis of Dendronized Diblock Copolymers via Ring-Opening Metathesis Polymerization and Their Visualization Using Atomic Force Microscopy. *J. Am. Chem. Soc.* **2007**, *129*, 9619–9621. https://doi.org/10.1145/1961678.1961690.

(89) Jung, H.; Carberry, T. P.; Weck, M. Synthesis of First- and Second-Generation Poly(Amide)-Dendronized Polymers via Ring-Opening Metathesis Polymerization. *Macromolecules* **2011**, *44* (23), 9075–9083. https://doi.org/10.1021/ma2016375.

(90) Kim, K. O.; Choi, T.-L. Synthesis of Rod-Like Dendronized Polymers Containing G4 and G5 Ester Dendrons via Macromonomer Approach by Living ROMP. *ACS Macro Lett.* **2012**, *1* (4), 445–448. https://doi.org/10.1021/mz300032w.

(91) Dutertre, F.; Bang, K.-T.; Vereroudakis, E.; Loppinet, B.; Yang, S.; Kang, S.-Y.; Fytas, G.; Choi, T.-L. Conformation of Tunable Nanocylinders: Up to Sixth-Generation Dendronized Polymers via Graft-Through Approach by ROMP. *Macromolecules* **2019**, *52* (9), 3342–3350. https://doi.org/10.1021/acs.macromol.9b00457.

(92) Piunova, V. A.; Miyake, G. M.; Daeffler, C. S.; Weitekamp, R. A.; Grubbs, R. H. Highly Ordered Dielectric Mirrors via the Self-Assembly of Dendronized Block Copolymers. *J. Am. Chem. Soc.* **2013**, *135* (41), 15609–15616. https://doi.org/10.1021/ja4081502.

(93) Kim, K. O.; Shin, S.; Kim, J.; Choi, T.-L. Living Polymerization of Monomers Containing *Endo* -Tricyclo[4.2.2.0 ^{2,5}]Deca-3,9-Diene Using Second Generation Grubbs and Hoveyda–Grubbs Catalysts: Approach to Synthesis of Well-Defined Star Polymers. *Macromolecules* **2014**, *47* (4), 1351–1359. https://doi.org/10.1021/ma5000333.

(94) Liu, X.; Qiu, G.; Zhang, L.; Liu, F.; Mu, S.; Long, Y.; Zhao, Q.; Liu, Y.; Gu, H. Controlled ROMP Synthesis of Ferrocene-Containing Amphiphilic Dendronized Diblock Copolymers as Redox-Controlled Polymer Carriers. *Macromol. Chem. Phys.* **2018**, *219* (18), 1800273. https://doi.org/10.1002/macp.201800273.

(95) Liu, X.; Ling, Q.; Zhao, L.; Qiu, G.; Wang, Y.; Song, L.; Zhang, Y.; Ruiz, J.; Astruc, D.; Gu, H. New ROMP Synthesis of Ferrocenyl Dendronized Polymers. *Macromol. Rapid Commun.* **2017**, *38* (19), 1700448. https://doi.org/10.1002/marc.201700448.

(96) Chulu Zhou, C. H., Wei Chen, Lijie Wang, Jianhua Cheng. Progress of Application of Ring-Opening Metathesis Polymerization (ROMP) in the Synthesis of Star Polymers. *Acta Chim. Sin.* **2022**, *80* (2), 229–236.

(97) Bazan, G. C.; Schrock, R. R. Synthesis of Star Block Copolymers by Controlled Ring-Opening Metathesis Polymerization. *Macromolecules* **1991**, *24* (4), 817–823. https://doi.org/10.1021/ma00004a001.

(98) Saunders, R. S.; Cohen, R. E.; Wong, S. J.; Schrock, R. R. Synthesis of Amphiphilic Star Block Copolymers Using Ring-Opening Metathesis Polymerization. *Macromolecules* **1992**, *25* (7), 2055–2057. https://doi.org/10.1021/ma00033a035.

(99) Nomura, K.; Watanabe, Y.; Fujita, S.; Fujiki, M.; Otani, H. Facile Controlled Synthesis of Soluble Star Shape Polymers by Ring-Opening Metathesis Polymerization (ROMP). *Macromolecules* **2009**, *42* (4), 899–901. https://doi.org/10.1021/ma8027529.

(100) Teo, Y. C.; Lai, H. W. H.; Xia, Y. Arm-Degradable Star Polymers with Crosslinked Ladder-Motif Cores as a Route to Soluble Microporous Nanoparticles. *Polym. Chem.* **2020**, *11* (2), 265–269. https://doi.org/10.1039/C9PY01060B.

(101) Liu, J.; Li, J.; Xie, M.; Ding, L.; Yang, D.; Zhang, L. A Novel Amphiphilic AB 2 Star Copolymer Synthesized by the Combination of Ring-Opening Metathesis Polymerization and Atom Transfer Radical Polymerization. *Polymer* **2009**, *50*, 5228–5235. https://doi.org/10.1016/j.polymer.2009.09.029.

(102) Levi, A. E.; Fu, L.; Lequieu, J.; Horne, J. D.; Blankenship, J.; Mukherjee, S.; Zhang, T.; Fredrickson, G. H.; Gutekunst, W. R.; Bates, C. M. Efficient Synthesis of Asymmetric Miktoarm Star Polymers. *Macromolecules* **2020**, *53* (2), 702–710. https://doi.org/10.1021/acs.macromol.9b02380.

(103) Liu, J.; Burts, A. O.; Li, Y.; Zhukhovitskiy, A. V.; Ottaviani, M. F.; Turro, N. J.; Johnson, J. A. "Brush-First" Method for the Parallel Synthesis of Photocleavable, Nitroxide-Labeled Poly(Ethylene Glycol) Star Polymers. *J. Am. Chem. Soc.* **2012**, *134* (39), 16337–16344. https://doi.org/10.1021/ja3067176.

(104) Burts, A. O.; Gao, A. X.; Johnson, J. A. Brush-First Synthesis of Core-Photodegradable Miktoarm Star Polymers via ROMP: Towards Photoresponsive Self-Assemblies. *Macromol. Rapid Commun.* **2014**, *35* (2), 168–173. https://doi.org/10.1002/marc.201300618.

(105) Burts, A. O.; Liao, L.; Lu, Y. Y.; Tirrell, D. A.; Johnson, J. A. Brush-First and Click: Efficient Synthesis of Nanoparticles That Degrade and Release Doxorubicin in Response to Light. *Photochem. Photobiol.* **2014**, *90* (2), 380–385. https://doi.org/10.1111/php.12182.

(106) Gao, A. X.; Liao, L.; Johnson, J. A. Synthesis of Acid-Labile PEG and PEG-Doxorubicin-Conjugate Nanoparticles via Brush-First ROMP. *ACS Macro Lett.* **2014**, *3* (9), 854–857. https://doi.org/10.1021/mz5004097.

(107) Li, R.; Li, X.; Zhang, Y.; Delawder, A. O.; Colley, N. D.; Whiting, E. A.; Barnes, J. C. Diblock Brush-Arm Star Copolymers via a Core-First/Graft-from Approach Using γ-Cyclodextrin and ROMP: A Modular Platform for Drug Delivery. *Polym. Chem.* **2020**, *11* (2), 541–550. https://doi.org/10.1039/C9PY01146C.

(108) Beerens, H.; Wang, W.; Verdonck, L.; Verpoort, F. Multi-Nuclear Dendritic Ru-Complexes as Catalysts for ROMP; Synthesis and Characterization of Starpolymers. *15th Int. Symp. Olefin Metathesis Relat. Chem.* **2002**, *190* (1), 1–7. https://doi.org/10.1016/S1381-1169(02)00224-8.

(109) Gauthier, M. A.; Klok, H.-A. Polymer–Protein Conjugates: An Enzymatic Activity Perspective. *Polym. Chem.* **2010**, *1* (9), 1352–1373. https://doi.org/10.1039/C0PY90001J.

(110) Maynard, H. D.; Okada, S. Y.; Grubbs, R. H. Inhibition of Cell Adhesion to Fibronectin by Oligopeptide-Substituted Polynorbornenes. *J. Am. Chem. Soc.* **2001**, *123* (7), 1275–1279. https://doi.org/10.1021/ja003305m.

(111) Hahn, M. E.; Randolph, L. M.; Adamiak, L.; Thompson, M. P.; Gianneschi, N. C. Polymerization of a Peptide-Based Enzyme Substrate. *Chem. Commun.* **2013**, *49* (28), 2873. https://doi.org/10.1039/c3cc40472b.

(112) Kammeyer, J. K.; Blum, A. P.; Adamiak, L.; Hahn, M. E.; Gianneschi, N. C. Polymerization of Protecting-Group-Free Peptides via ROMP. *Polym. Chem.* **2013**, *4* (14), 3929. https://doi.org/10.1039/c3py00526g.

(113) Messina, M. S.; Messina, K. M. M.; Bhattacharya, A.; Montgomery, H. R.; Maynard, H. D. Preparation of Biomolecule-Polymer Conjugates by Grafting-from Using ATRP, RAFT, or ROMP. *Prog. Polym. Sci.* **2020**, *100*, 101186. https://doi.org/10.1016/j.progpolymsci.2019.101186.

(114) Jevsevar, S.; Kunstelj, M.; Porekar, V. G. PEGylation of Therapeutic Proteins. *Biotechnol. J.* **2010**, *5* (1), 113–128. https://doi.org/10.1002/biot.200900218.

(115) Isarov, S. A.; Pokorski, J. K. Protein ROMP: Aqueous Graft-from Ring-Opening Metathesis Polymerization. *ACS Macro Lett.* **2015**, *4* (9), 969–973. https://doi.org/10.1021/acsmacrolett.5b00497.

(116) Isarov, S. A.; Lee, P. W.; Pokorski, J. K. "Graft-to" Protein/Polymer Conjugates Using Polynorbornene Block Copolymers. *Biomacromolecules* **2016**, *17* (2), 641–648. https://doi.org/10.1021/acs.biomac.5b01582.

(117) Lu, X.; Watts, E.; Jia, F.; Tan, X.; Zhang, K. Polycondensation of Polymer Brushes via DNA Hybridization. *J. Am. Chem. Soc.* **2014**, *136* (29), 10214–10217. https://doi.org/10.1021/ja504790r.

(118) Tan, X.; Lu, H.; Sun, Y.; Chen, X.; Wang, D.; Jia, F.; Zhang, K. Expanding the Materials Space of DNA via Organic-Phase Ring-Opening Metathesis Polymerization. *Chem* **2019**, *5* (6), 1584–1596. https://doi.org/10.1016/j.chempr.2019.03.023.

(119) Tsukahara, Y.; Namba, S.; Iwasa, J.; Nakano, Y.; Kaeriyama, K.; Takahashi, M. Bulk Properties of Poly(Macromonomer)s of Increased Backbone and Branch Lengths. *Macromolecules* **2001**, *34*, 2624–2629.

(120) Arrington, K. J.; Radzinski, S. C.; Drummey, K. J.; Long, T. E.; Matson, J. B. Reversibly Cross-Linkable Bottlebrush Polymers as Pressure-Sensitive Adhesives. *ACS Appl. Mater. Interfaces* **2018**, *10* (31), 26662–26668. https://doi.org/10.1021/acsami.8b08480.

(121) Li, X.; Prukop, S. L.; Biswal, S. L.; Verduzco, R. Surface Properties of Bottlebrush Polymer Thin Films. *Macromolecules* **2012**, *45*, 7118–7127.

(122) Daniel, W. F. M.; Burdynska, J.; Vatankhah-Varnoosfaderani, M.; Matyjaszewski, K.; Paturej, J.; Rubinstein, M.; Dobrynin, A. V.; Sheiko, S. S. Solvent-Free, Supersoft and Superelastic Bottlebrush Melts and Networks. *Nat. Mater.* **2016**, *15*, 8.

(123) Paturej, J. Molecular Structure of Bottlebrush Polymers in Melts. *Sci. Adv.* **2016**, *2*, 1–12.

(124) Noel, A.; Borguet, Y. P.; Wooley, K. L. Self-Reporting Degradable Fluorescent Grafted Copolymer Micelles Derived from Biorenewable Resources. *ACS Macro Lett.* **2015**, 6.

(125) Ohno, S.; Matyjaszewski, K. Controlling Grafting Density and Side Chain Length in Poly(*n* -Butyl Acrylate) by ATRP Copolymerization of Macromonomers. *J. Polym. Sci. Part Polym. Chem.* **2006**, *44*, 5454–5467.

(126) Satoh, K.; Matsuda, M.; Nagai, K.; Kamigaito, M. AAB-Sequence Living Radical Chain Copolymerization of Naturally Occurring Limonene with Maleimide: An End-to-End Sequence-Regulated Copolymer. *J. Am. Chem. Soc.* **2010**, *132*, 10003–10005. https://doi.org/10.1021/ja1042353.

(127) Lin, T.-P.; Chang, A. B.; Chen, H.-Y.; Liberman-Martin, A. L.; Bates, C. M.; Voegtle, M. J.; Bauer, C. A.; Grubbs, R. H. Control of Grafting Density and Distribution in Graft Polymers by Living Ring-Opening Metathesis Copolymerization. *J. Am. Chem. Soc.* **2017**, *139* (10), 3896–3903. https://doi.org/10.1021/jacs.7b00791.

(128) Lin, T.-P.; Chang, A. B.; Luo, S.-X.; Chen, H.-Y.; Lee, B.; Grubbs, R. H. Effects of Grafting Density on Block Polymer Self-Assembly: From Linear to Bottlebrush. *ACS Nano* **2017**, *11* (11), 11632–11641. https://doi.org/10.1021/acsnano.7b06664.

(129) Jiang, L.; Nykypanchuk, D.; Ribbe, A. E.; Rzayev, J. One-Shot Synthesis and Melt Self-Assembly of Bottlebrush Copolymers with a Gradient Compositional Profile. *ACS Macro Lett.* **2018**, *7* (6), 619–623. https://doi.org/10.1021/acsmacrolett.8b00273.

(130) Jiang, L.; Nykypanchuk, D.; Pastore, V. J.; Rzayev, J. Morphological Behavior of Compositionally Gradient Polystyrene–Polylactide Bottlebrush Copolymers. *Macromolecules* **2019**, *52*, 8217–8226.

(131) Stuart, M. A. C.; Huck, W. T. S.; Genzer, J.; Müller, M.; Ober, C.; Stamm, M.; Sukhorukov, G. B.; Szleifer, I.; Tsukruk, V. V.; Urban, M.; Winnik, F.; Zauscher, S.; Luzinov, I.; Minko, S. Emerging Applications of Stimuli-Responsive Polymer Materials. *Nat. Mater.* **2010**, *9* (2), 101–113. https://doi.org/10.1038/nmat2614.

(132) Sun, H.; Kabb, C. P.; Dai, Y.; Hill, M. R.; Ghiviriga, I.; Bapat, A. P.; Sumerlin, B. S. Macromolecular Metamorphosis via Stimulus-Induced Transformations of Polymer Architecture. *Nat. Chem.* **2017**, *9* (8), 817–823. https://doi.org/10.1038/nchem.2730.

(133) Neary, W. J.; Isais, T. A.; Kennemur, J. G. Depolymerization of Bottlebrush Polypentenamers and Their Macromolecular Metamorphosis. *J. Am. Chem. Soc.* **2019**, *141* (36), 14220–14229. https://doi.org/10.1021/jacs.9b05560.

(134) Neary, W. J.; Kennemur, J. G. Variable Temperature ROMP: Leveraging Low Ring Strain Thermodynamics To Achieve Well-Defined Polypentenamers. *Macromolecules* **2017**, *50* (13), 4935–4941. https://doi.org/10.1021/acs.macromol.7b01148.

(135) Neary, W. J.; Fultz, B. A.; Kennemur, J. G. Well-Defined and Precision-Grafted Bottlebrush Polypentenamers from Variable Temperature ROMP and ATRP. *ACS Macro Lett.* **2018**, *7* (9), 1080–1086. https://doi.org/10.1021/acsmacrolett.8b00576.

(136) Bielawski, C. W.; Benitez, D.; Morita, T.; Grubbs, R. H. Synthesis of End-Functionalized Poly(Norbornene)s via Ring-Opening Metathesis Polymerization. *Macromolecules* **2001**, *34* (25), 8610–8618. https://doi.org/10.1021/ma010878q.

(137) Liu, P.; Yasir, M.; Ruggi, A.; Kilbinger, A. F. M. Heterotelechelic Polymers by Ring-Opening Metathesis and Regioselective Chain Transfer. *Angew. Chem. Int. Ed.* **2018**, *57* (4), 914–917. https://doi.org/10.1002/anie.201708733.

(138) Matson, J. B.; Virgil, S. C.; Grubbs, R. H. Pulsed-Addition Ring-Opening Metathesis Polymerization: Catalyst-Economical Syntheses of Homopolymers and Block Copolymers. *J. Am. Chem. Soc.* **2009**, *131* (9), 3355–3362. https://doi.org/10.1021/ja809081h.

(139) Yasir, M.; Liu, P.; Tennie, I. K.; Kilbinger, A. F. M. Catalytic Living Ring-Opening Metathesis Polymerization with Grubbs' Second- and Third-Generation Catalysts. *Nat. Chem.* **2019**, *11* (5), 488–494. https://doi.org/10.1038/s41557-019-0239-4.

(140) Sutthasupa, S.; Shiotsuki, M.; Sanda, F. Recent Advances in Ring-Opening Metathesis Polymerization, and Application to Synthesis of Functional Materials. *Polym. J.* **2010**, *42* (12), 905–915. https://doi.org/10.1038/pj.2010.94.

(141) Smith, D.; Pentzer, E. B.; Nguyen, S. T. Bioactive and Therapeutic ROMP Polymers. *J. Macromol. Sci. Part C Polym. Rev.* **2007**, *47* (3), 419–459.

(142) Buchmeiser, M. R. Ring-Opening Metathesis Polymerization-Derived Materials for Separation Science, Heterogeneous Catalysis and Tissue Engineering. *Macromol. Symp.* **2010**, *298* (1), 17–24. https://doi.org/10.1002/masy.201000014.

(143) Hollauf, M.; Trimmel, G.; Knall, A.-C. Dye-Functionalized Polymers via Ring Opening Metathesis Polymerization: Principal Routes and Applications. *Monatshefte Für Chem. - Chem. Mon.* **2015**, *146* (7), 1063–1080. https://doi.org/10.1007/s00706-015-1493-9.

(144) Liu, P.; Ai, C. Olefin Metathesis Reaction in Rubber Chemistry and Industry and Beyond. *Ind. Eng. Chem. Res.* **2018**, *57* (11), 3807–3820. https://doi.org/10.1021/acs.iecr.7b03830.

(145) Sveinbjörnsson, B. R.; Weitekamp, R. A.; Miyake, G. M.; Xia, Y.; Atwater, H. A.; Grubbs, R. H. Rapid Self-Assembly of Brush Block Copolymers to Photonic Crystals. *Proceedings of the National Academy of Sciences*, 2012, *109*, 14332–14336.

(146) Macfarlane, R. J.; Kim, B.; Lee, B.; Weitekamp, R. A.; Bates, C. M.; Lee, S. F.; Chang, A. B.; Delaney, K. T.; Fredrickson, G. H.; Atwater, H. A.; Grubbs, R. H. Improving Brush Polymer Infrared One-Dimensional Photonic Crystals via Linear Polymer Additives. *J. Am. Chem. Soc.* **2014**, *136* (50), 17374–17377. https://doi.org/10.1021/ja5093562.

(147) Miyake, G. M.; Piunova, V. A.; Weitekamp, R. A.; Grubbs, R. H. Precisely Tunable Photonic Crystals From Rapidly Self-Assembling Brush Block Copolymer Blends. *Angew. Chem. Int. Ed.* **2012**, *51* (45), 11246–11248. https://doi.org/10.1002/anie.201205743.

(148) Miyake, G. M.; Weitekamp, R. A.; Piunova, V. A.; Grubbs, R. H. Synthesis of Isocyanate-Based Brush Block Copolymers and Their Rapid Self-Assembly to Infrared-Reflecting Photonic Crystals. *J. Am. Chem. Soc.* **2012**, *134* (34), 14249–14254. https://doi.org/10.1021/ja306430k.

(149) Guo, T.; Wang, Y.; Qiao, Y.; Yuan, X.; Zhao, Y.; Ren, L. Thermal Property of Photonic Crystals (PCs) Prepared by Solvent Annealing Self-Assembly of Bottlebrush PS-b-PtBA. *Polymer* **2020**, *194*, 122389. https://doi.org/10.1016/j.polymer.2020.122389.

(150) Yu, Y.-G.; Seo, C.; Chae, C.-G.; Seo, H.-B.; Kim, M.-J.; Kang, Y.; Lee, J.-S. Hydrogen Bonding-Mediated Phase Transition of Polystyrene and Polyhydroxystyrene Bottlebrush Block Copolymers with Polyethylene Glycol. *Macromolecules* **2019**, *52* (11), 4349–4358. https://doi.org/10.1021/acs.macromol.9b00678.

(151) Song, D.-P.; Li, C.; Colella, N. S.; Lu, X.; Lee, J.-H.; Watkins, J. J. Thermally Tunable Metallodielectric Photonic Crystals from the Self-Assembly of Brush Block Copolymers and Gold Nanoparticles. *Adv. Opt. Mater.* **2015**, *3* (9), 1169–1175. https://doi.org/10.1002/adom.201500116.

(152) Song, D.-P.; Li, C.; Li, W.; Watkins, J. J. Block Copolymer Nanocomposites with High Refractive Index Contrast for One-Step Photonics. *ACS Nano* **2016**, *10* (1), 1216–1223. https://doi.org/10.1021/acsnano.5b06525.

(153) Song, D.-P.; Zhao, T. H.; Guidetti, G.; Vignolini, S.; Parker, R. M. Hierarchical Photonic Pigments via the Confined Self-Assembly of Bottlebrush Block Copolymers. *ACS Nano* **2019**, *13* (2), 1764–1771. https://doi.org/10.1021/acsnano.8b07845.

(154) Patel Bijal B.; Walsh Dylan J.; Kim Do Hoon; Kwok Justin; Lee Byeongdu; Guironnet Damien; Diao Ying. Tunable Structural Color of Bottlebrush Block Copolymers through Direct-Write 3D Printing from Solution. *Sci. Adv. 6* (24), eaaz7202. https://doi.org/10.1126/sciadv.aaz7202.

(155) Miki, K.; Kimura, A.; Oride, K.; Kuramochi, Y.; Matsuoka, H.; Harada, H.; Hiraoka, M.; Ohe, K. High-Contrast Fluorescence Imaging of Tumors In Vivo Using Nanoparticles of Amphiphilic Brush-Like Copolymers Produced by ROMP. *Angew. Chem. Int. Ed.* **2011**, *50* (29), 6567–6570. https://doi.org/10.1002/anie.201101005.

(156) Rajca, A.; Wang, Y.; Boska, M.; Paletta, J. T.; Olankitwanit, A.; Swanson, M. A.; Mitchell, D. G.; Eaton, S. S.; Eaton, G. R.; Rajca, S. Organic Radical Contrast Agents for Magnetic Resonance Imaging. *J. Am. Chem. Soc.* **2012**, *134* (38), 15724–15727. https://doi.org/10.1021/ja3079829.

(157) Sankaran, N. B.; Rys, A. Z.; Nassif, R.; Nayak, M. K.; Metera, K.; Chen, B.; Bazzi, H. S.; Sleiman, H. F. Ring-Opening Metathesis Polymers for Biodetection and Signal Amplification: Synthesis and Self-Assembly. *Macromolecules* **2010**, *43* (13), 5530–5537. https://doi.org/10.1021/ma100234j.

(158) Fouz, M. F.; Mukumoto, K.; Averick, S.; Molinar, O.; McCartney, B. M.; Matyjaszewski, K.; Armitage, B. A.; Das, S. R. Bright Fluorescent Nanotags from Bottlebrush Polymers with DNA-Tipped Bristles. *ACS Cent. Sci.* **2015**, *1* (8), 431–438. https://doi.org/10.1021/acscentsci.5b00259.

(159) Sowers, M. A.; McCombs, J. R.; Wang, Y.; Paletta, J. T.; Morton, S. W.; Dreaden, E. C.; Boska, M. D.; Ottaviani, M. F.; Hammond, P. T.; Rajca, A.; Johnson, J. A. Redox-Responsive Branched-Bottlebrush Polymers for in Vivo MRI and Fluorescence Imaging. *Nat. Commun.* **2014**, *5* (1), 5460. https://doi.org/10.1038/ncomms6460.

(160) Zeng, X.; Wang, L.; Liu, D.; Liu, D. Poly(L-Lysine)-Based Cylindrical Copolypeptide Brushes as Potential Drug and Gene Carriers. *Colloid Polym. Sci.* **2016**, *294* (12), 1909–1920. https://doi.org/10.1007/s00396-016-3953-0.

(161) Zhao, P.; Liu, L.; Feng, X.; Wang, C.; Shuai, X.; Chen, Y. Molecular Nanoworm with PCL Core and PEO Shell as a Non-Spherical Carrier for Drug Delivery. *Macromol. Rapid Commun.* **2012**, *33* (16), 1351–1355. https://doi.org/10.1002/marc.201200172.

(162) Müllner, M.; Yang, K.; Kaur, A.; New, E. J. Aspect-Ratio-Dependent Interaction of Molecular Polymer Brushes and Multicellular Tumour Spheroids. *Polym. Chem.* **2018**, *9* (25), 3461–3465. https://doi.org/10.1039/C8PY00703A.

(163) Johnson, J. A.; Lu, Y. Y.; Burts, A. O.; Xia, Y.; Durrell, A. C.; Tirrell, D. A.; Grubbs, R. H. Drug-Loaded, Bivalent-Bottle-Brush Polymers by Graft-through ROMP. *Macromolecules* **2010**, *43* (24), 10326–10335. https://doi.org/10.1021/ma1021506.

(164) Powell, C. R.; Kaur, K.; Dillon, K. M.; Zhou, M.; Alaboalirat, M.; Matson, J. B. Functional N-Substituted N-Thiocarboxyanhydrides as Modular Tools for Constructing H2S Donor Conjugates. *ACS Chem. Biol.* **2019**, *14* (6), 1129–1134. https://doi.org/10.1021/acschembio.9b00248.

(165) Liao, L.; Liu, J.; Dreaden, E. C.; Morton, S. W.; Shopsowitz, K. E.; Hammond, P. T.; Johnson, J. A. A Convergent Synthetic Platform for Single-Nanoparticle Combination Cancer Therapy: Ratiometric Loading and Controlled Release of Cisplatin, Doxorubicin, and Camptothecin. *J. Am. Chem. Soc.* **2014**, *136* (16), 5896–5899. https://doi.org/10.1021/ja502011g.

(166) Pelras, T.; Mahon, C. S.; Nonappa; Ikkala, O.; Gröschel, A. H.; Müllner, M. Polymer Nanowires with Highly Precise Internal Morphology and Topography. *J. Am. Chem. Soc.* **2018**, *140* (40), 12736–12740. https://doi.org/10.1021/jacs.8b08870.

(167) Tonge, C. M.; Sauvé, E. R.; Cheng, S.; Howard, T. A.; Hudson, Z. M. Multiblock Bottlebrush Nanofibers from Organic Electronic Materials. *J. Am. Chem. Soc.* **2018**, *140* (37), 11599–11603. https://doi.org/10.1021/jacs.8b07915.

(168) Tonge, C. M.; Hudson, Z. M. Interface-Dependent Aggregation-Induced Delayed Fluorescence in Bottlebrush Polymer Nanofibers. *J. Am. Chem. Soc.* **2019**, *141* (35), 13970–13976. https://doi.org/10.1021/jacs.9b07156.

(169) Daniel, W. F. M.; Burdyńska, J.; Vatankhah-Varnoosfaderani, M.; Matyjaszewski, K.; Paturej, J.; Rubinstein, M.; Dobrynin, A. V.; Sheiko, S. S. Solvent-Free, Supersoft and Superelastic Bottlebrush Melts and Networks. *Nat. Mater.* **2016**, *15* (2), 183–189. https://doi.org/10.1038/nmat4508.

(170) Pakula, T.; Zhang, Y.; Matyjaszewski, K.; Lee, H.; Boerner, H.; Qin, S.; Berry, G. C. Molecular Brushes as Super-Soft Elastomers. *Contain. Struct. Dyn. Complex Polym. Mater. Commem. Tadeusz Pakula* **2006**, *47* (20), 7198–7206. https://doi.org/10.1016/j.polymer.2006.05.064.

(171) Slegeris, R.; Ondrusek, B. A.; Chung, H. Catechol- and Ketone-Containing Multifunctional Bottlebrush Polymers for Oxime Ligation and Hydrogel Formation. *Polym. Chem.* **2017**, *8* (32), 4707–4715. https://doi.org/10.1039/C7PY01112A.

(172) Alaboalirat, M.; Matson, J. B. Poly(β-Cyclodextrin) Prepared by Ring-Opening Metathesis Polymerization Enables Creation of Supramolecular Polymeric Networks. *ACS Macro Lett.* **2021**, 1460–1466. https://doi.org/10.1021/acsmacrolett.1c00590.

(173) Cai, L.-H.; Kodger, T. E.; Guerra, R. E.; Pegoraro, A. F.; Rubinstein, M.; Weitz, D. A. Soft Poly(Dimethylsiloxane) Elastomers from Architecture-Driven Entanglement Free Design. *Adv. Mater.* **2015**, *27* (35), 5132–5140. https://doi.org/10.1002/adma.201502771.

(174) Sarapas, J. M.; Chan, E. P.; Rettner, E. M.; Beers, K. L. Compressing and Swelling To Study the Structure of Extremely Soft Bottlebrush Networks Prepared by ROMP. *Macromolecules* **2018**, *51* (6), 2359–2366. https://doi.org/10.1021/acs.macromol.8b00018.

(175) Reynolds, V. G.; Mukherjee, S.; Xie, R.; Levi, A. E.; Atassi, A.; Uchiyama, T.; Wang, H.; Chabinyc, M. L.; Bates, C. M. Super-Soft Solvent-Free Bottlebrush Elastomers for Touch Sensing. *Mater. Horiz.* **2020**, *7* (1), 181–187. https://doi.org/10.1039/C9MH00951E.

(176) Mukherjee, S.; Xie, R.; Reynolds, V. G.; Uchiyama, T.; Levi, A. E.; Valois, E.; Wang, H.; Chabinyc, M. L.; Bates, C. M. Universal Approach to Photo-Crosslink Bottlebrush Polymers. *Macromolecules* **2020**, *53* (3), 1090–1097. https://doi.org/10.1021/acs.macromol.9b02210.

(177) Nian, S.; Lian, H.; Gong, Z.; Zhernenkov, M.; Qin, J.; Cai, L.-H. Molecular Architecture Directs Linear–Bottlebrush–Linear Triblock Copolymers to Self-Assemble to Soft Reprocessable Elastomers. *ACS Macro Lett.* **2019**, *8* (11), 1528–1534. https://doi.org/10.1021/acsmacrolett.9b00721.

(178) Clair, C.; Lallam, A.; Rosenthal, M.; Sztucki, M.; Vatankhah-Varnosfaderani, M.; Keith, A. N.; Cong, Y.; Liang, H.; Dobrynin, A. V.; Sheiko, S. S.; Ivanov, D. A. Strained Bottlebrushes in Super-Soft Physical Networks. *ACS Macro Lett.* **2019**, *8* (5), 530–534. https://doi.org/10.1021/acsmacrolett.9b00106.

(179) Keith, A. N.; Vatankhah-Varnosfaderani, M.; Clair, C.; Fahimipour, F.; Dashtimoghadam, E.; Lallam, A.; Sztucki, M.; Ivanov, D. A.; Liang, H.; Dobrynin, A. V.; Sheiko, S. S. Bottlebrush Bridge between Soft Gels and Firm Tissues. *ACS Cent. Sci.* **2020**, *6* (3), 413–419. https://doi.org/10.1021/acscentsci.9b01216.

(180) Self, J. L.; Sample, C. S.; Levi, A. E.; Li, K.; Xie, R.; de Alaniz, J. R.; Bates, C. M. Dynamic Bottlebrush Polymer Networks: Self-Healing in Super-Soft Materials. *J. Am. Chem. Soc.* **2020**, *142* (16), 7567–7573. https://doi.org/10.1021/jacs.0c01467.

(181) Ahn, S.; Carrillo, J.-M. Y.; Keum, J. K.; Chen, J.; Uhrig, D.; Lokitz, B. S.; Sumpter, B. G.; Michael Kilbey, S. Nanoporous Poly(3-Hexylthiophene) Thin Film Structures from Self-Organization of a Tunable Molecular Bottlebrush Scaffold. *Nanoscale* **2017**, *9* (21), 7071–7080. https://doi.org/10.1039/C7NR00015D.

(182) Cho, S.; Son, J.; Kim, I.; Ahn, H.; Jang, H.-S.; Joo, S. H.; Park, K. H.; Lee, E.; Kim, Y.; Ahn, S. Asymmetric Polystyrene-Polylactide Bottlebrush Random Copolymers: Synthesis, Self-Assembly

and Nanoporous Structures. *Polymer* **2019**, *175*, 49–56. https://doi.org/10.1016/j.polymer.2019.04.075.

(183) Chae, C.-G.; Yu, Y.-G.; Seo, H.-B.; Kim, M.-J.; Mallela, Y. L. N. K.; Lee, J.-S. Molecular Design of an Interfacially Active POSS-Bottlebrush Block Copolymer for the Fabrication of Three-Dimensional Porous Films with Unimodal Pore Size Distributions through the Breath-Figure Self-Assembly. *Macromolecules* **2019**, *52* (5), 1912–1922. https://doi.org/10.1021/acs.macromol.9b00089.

(184) Li, Y.-L.; Chen, X.; Geng, H.-K.; Dong, Y.; Wang, B.; Ma, Z.; Pan, L.; Ma, G.-Q.; Song, D.-P.; Li, Y.-S. Oxidation Control of Bottlebrush Molecular Conformation for Producing Libraries of Photonic Structures. *Angew. Chem. Int. Ed.* **2021**, *60* (7), 3647–3653. https://doi.org/10.1002/anie.202011702.

(185) Huang, K.; Rzayev, J. Well-Defined Organic Nanotubes from Multicomponent Bottlebrush Copolymers. *J. Am. Chem. Soc.* **2009**, *131* (19), 6880–6885. https://doi.org/10.1021/ja901936g.

(186) Xia, X.; Bass, G.; Becker, M. L.; Vogt, B. D. Tuning Cooperative Assembly with Bottlebrush Block Co-Polymers for Porous Metal Oxide Films Using Solvent Mixtures. *Langmuir* **2019**, *35* (29), 9572–9583. https://doi.org/10.1021/acs.langmuir.9b01363.

(187) Altay, E.; Nykypanchuk, D.; Rzayev, J. Mesoporous Polymer Frameworks from End-Reactive Bottlebrush Copolymers. *ACS Nano* **2017**, *11* (8), 8207–8214. https://doi.org/10.1021/acsnano.7b03214.

(188) Fei, H.-F.; Li, W.; Nuguri, S.; Yu, H.-J.; Yavitt, B. M.; Fan, W.; Watkins, J. J. One-Step Synthesis of Hierarchical, Bimodal Nanoporous Carbons via Co-Templating with Bottlebrush and Linear Block Copolymers. *Chem. Mater.* **2020**, *32* (14), 6055–6061. https://doi.org/10.1021/acs.chemmater.0c01471.

(189) Chen, X.; Yang, X.; Song, D.-P.; Men, Y.-F.; Li, Y. Discovery and Insights into Organized Spontaneous Emulsification via Interfacial Self-Assembly of Amphiphilic Bottlebrush Block Copolymers. *Macromolecules* **2021**, *54* (8), 3668–3677. https://doi.org/10.1021/acs.macromol.1c00198.

(190) Kim, M.-J.; Yu, Y.-G.; Chae, C.-G.; Seo, H.-B.; Lee, J.-S. Facile Synthesis of Amphiphilic Bottlebrush Block Copolymers Bearing Pyridine Pendants via Click Reaction from Protected Alkyne Side Groups. *Macromolecules* **2020**, *53* (6), 2209–2219. https://doi.org/10.1021/acs.macromol.9b02674.

(191) Ji, E.; Cummins, C.; Fleury, G. Precise Synthesis and Thin Film Self-Assembly of PLLA-b-PS Bottlebrush Block Copolymers. *Molecules* **2021**, *26* (5). https://doi.org/10.3390/molecules26051412.

(192) Fei, H.-F.; Li, W.; Bhardwaj, A.; Nuguri, S.; Ribbe, A.; Watkins, J. J. Ordered Nanoporous Carbons with Broadly Tunable Pore Size Using Bottlebrush Block Copolymer Templates. *J. Am. Chem. Soc.* **2019**, *141* (42), 17006–17014. https://doi.org/10.1021/jacs.9b09572.

(193) Truong, N. P.; Whittaker, M. R.; Mak, C. W.; Davis, T. P. The Importance of Nanoparticle Shape in Cancer Drug Delivery. *Expert Opin. Drug Deliv.* **2015**, *12* (1), 129–142. https://doi.org/10.1517/17425247.2014.950564.

(194) Neugebauer, D.; Zhang, Y.; Pakula, T.; Sheiko, S. S.; Matyjaszewski, K. Densely-Grafted and Double-Grafted PEO Brushes via ATRP. A Route to Soft Elastomers. *Macromolecules* **2003**, *36* (18), 6746–6755. https://doi.org/10.1021/ma0345347.

(195) Elling, B. R.; Xia, Y. Living Alternating Ring-Opening Metathesis Polymerization Based on Single Monomer Additions. *J. Am. Chem. Soc.* **2015**, *137* (31), 9922–9926. https://doi.org/10.1021/jacs.5b05497.

(196) Parker, K. A.; Sampson, N. S. Precision Synthesis of Alternating Copolymers via Ring-Opening Polymerization of 1-Substituted Cyclobutenes. *Acc. Chem. Res.* **2016**, *49* (3), 408–417. https://doi.org/10.1021/acs.accounts.5b00490.

(197) Sanford, M. S.; Love, J. A.; Grubbs, R. H. A Versatile Precursor for the Synthesis of New Ruthenium Olefin Metathesis Catalysts. *Organometallics* **2001**, *20* (25), 5314–5318. https://doi.org/10.1021/om010599r.

(198) Choi, T.-L.; Grubbs, R. H. Controlled Living Ring-Opening-Metathesis Polymerization by a Fast-Initiating Ruthenium Catalyst. *Angew. Chem. Int. Ed.* **2003**, *42* (15), 1743–1746. https://doi.org/10.1002/anie.200250632.

(199) Scholl, M.; Ding, S.; Lee, C. W.; Grubbs, R. H. Synthesis and Activity of a New Generation of Ruthenium-Based Olefin Metathesis Catalysts Coordinated with 1,3-Dimesityl-4,5-Dihydroimidazol-2-Ylidene Ligands. *Org. Lett.* **1999**, *1* (6), 953–956. https://doi.org/10.1021/ol990909q.

(200) Diesendruck, C. E.; Vidavsky, Y.; Ben-Asuly, A.; Lemcoff, N. G. A Latent S-Chelated Ruthenium Benzylidene Initiator for Ring-Opening Metathesis Polymerization. *J. Polym. Sci. Part Polym. Chem.* **2009**, *47* (16), 4209–4213. https://doi.org/10.1002/pola.23476.

(201) McConville, D. H.; Wolf, J. R.; Schrock, R. R. Synthesis of Chiral Molybdenum ROMP Initiators and All-Cis Highly Tactic Poly(2,3-(R)2norbornadiene) (R = CF3 or CO2Me). *J. Am. Chem. Soc.* **1993**, *115* (10), 4413–4414. https://doi.org/10.1021/ja00063a090.

(202) Bielawski, C. W.; Grubbs, R. H. Living Ring-Opening Metathesis Polymerization. *50 Years Living Polym.* **2007**, *32* (1), 1–29. https://doi.org/10.1016/j.progpolymsci.2006.08.006.

(203) Ton, S. J.; Fogg, D. E. The Impact of Oxygen on Leading and Emerging Ru-Carbene Catalysts for Olefin Metathesis: An Unanticipated Correlation Between Robustness and Metathesis Activity. *ACS Catal.* **2019**, *9* (12), 11329–11334. https://doi.org/10.1021/acscatal.9b03285.

(204) Zhang, H.; Hadjichristidis, N. Well-Defined Bilayered Molecular Cobrushes with Internal Polyethylene Blocks and ω-Hydroxyl-Functionalized Polyethylene Homobrushes. *Macromolecules* **2016**, *49* (5), 1590–1596. https://doi.org/10.1021/acs.macromol.5b02652.

(205) Cazalis, C.; Héroguez, V.; Fontanille, M. Polymerizability of Cycloalkenes in a Living Ring-Opening Metathesis Polymerization Initiated by Schrock Complexes, 1. Effect of the Solvent on the Polymerization Kinetics. *Macromol. Chem. Phys.* **2000**, *201* (8), 869–876. https://doi.org/10.1002/(SICI)1521-3935(20000501)201:8<869::AID-MACP869>3.0.CO;2-Z.

(206) Ashworth, I. W.; Nelson, D. J.; Percy, J. M. Solvent Effects on Grubbs' Pre-Catalyst Initiation Rates. *Dalton Trans* **2013**, *42* (12), 4110–4113. https://doi.org/10.1039/C2DT32441E.

(207) Blosch, S. E.; Alaboalirat, M.; Eades, C. B.; Scannelli, S. J.; Matson, J. B. Solvent Effects in Grafting-through Ring-Opening Metathesis Polymerization. *Macromolecules* **2022**, *In press*. https://doi.org/10.1021/acs.macromol.2c00254.

(208) Hillmyer, M. A.; Lepetit, C.; McGrath, D. V.; Novak, B. M.; Grubbs, R. H. Aqueous Ring-Opening Metathesis Polymerization of Carboximide-Functionalized 7-Oxanorbornenes. *Macromolecules* **1992**, *25* (13), 3345–3350. https://doi.org/10.1021/ma00039a004.

(209) Rule, J. D.; Moore, J. S. ROMP Reactivity of Endo- and Exo-Dicyclopentadiene. *Macromolecules* **2002**, *35* (21), 7878–7882. https://doi.org/10.1021/ma0209489.

(210) Ivin, K. J.; Mol, J. C. *Olefin Metathesis and Metathesis Polymerization*; Elsevier Science, 1997.

(211) Pollino, J. M.; Stubbs, L. P.; Weck, M. Living ROMP of Exo-Norbornene Esters Possessing PdII SCS Pincer Complexes or Diaminopyridines. *Macromolecules* **2003**, *36* (7), 2230–2234. https://doi.org/10.1021/ma025873n.

(212) Moatsou, D.; Hansell, C. F.; O'Reilly, R. K. Precision Polymers: A Kinetic Approach for Functional Poly(Norbornenes). *Chem Sci* **2014**, *5* (6), 2246–2250. https://doi.org/10.1039/C4SC00752B.

(213) Pal, S.; Alizadeh, M.; Kong, P.; Kilbinger, A. F. M. Oxanorbornenes: Promising New Single Addition Monomers for the Metathesis Polymerization. *Chem. Sci.* **2021**, *12* (19), 6705–6711. https://doi.org/10.1039/D1SC00036E.

(214) Hyatt, M. G.; Walsh, D. J.; Lord, R. L.; Andino Martinez, J. G.; Guironnet, D. Mechanistic and Kinetic Studies of the Ring Opening Metathesis Polymerization of Norbornenyl Monomers by a Grubbs Third Generation Catalyst. *J. Am. Chem. Soc.* **2019**, *141* (44), 17918–17925. https://doi.org/10.1021/jacs.9b09752.

(215) Wolf, W. J.; Lin, T.-P.; Grubbs, R. H. Examining the Effects of Monomer and Catalyst Structure on the Mechanism of Ruthenium-Catalyzed Ring-Opening Metathesis Polymerization. *J. Am. Chem. Soc.* **2019**, *141* (44), 17796–17808. https://doi.org/10.1021/jacs.9b08835.

(216) Slugovc, C.; Demel, S.; Riegler, S.; Hobisch, J.; Stelzer, F. The Resting State Makes the Difference: The Influence of the Anchor Group in the ROMP of Norbornene Derivatives. *Macromol. Rapid Commun.* **2004**, *25* (3), 475–480. https://doi.org/10.1002/marc.200300196.

(217) Radzinski, S. C.; Foster, J. C.; Chapleski, R. C.; Troya, D.; Matson, J. B. Bottlebrush Polymer Synthesis by Ring-Opening Metathesis Polymerization: The Significance of the Anchor Group. *J. Am. Chem. Soc.* **2016**, *138* (22), 6998–7004. https://doi.org/10.1021/jacs.5b13317.

(218) Feast, W. J.; Gibson, V. C.; Johnson, A. F.; Khosravi, E.; Mohsin, M. A. Well-Defined Graft Copolymers via Coupled Living Anionic and Living Ring Opening Metathesis Polymerisation. *Int. Symp. Olefin Metathesis Relat. Chem.* **1997**, *115* (1), 37–42. https://doi.org/10.1016/S1381-1169(96)00078-7.

(219) Matyjaszewski, K. Ranking Living Systems. *Macromolecules* **1993**, *26* (7), 1787–1788. https://doi.org/10.1021/ma00059a048.

(220) Pesek, S. L.; Li, X.; Hammouda, B.; Hong, K.; Verduzco, R. Small-Angle Neutron Scattering Analysis of Bottlebrush Polymers Prepared via Grafting-through Polymerization. *Macromolecules* **2013**, *46* (17), 6998–7005.

(221) Ritter, T.; Hejl, A.; Wenzel, A. G.; Funk, T. W.; Grubbs, R. H. A Standard System of Characterization for Olefin Metathesis Catalysts. *Organometallics* **2006**, *25* (24), 5740–5745. https://doi.org/10.1021/om060520o.

(222) Feist, J. D.; Xia, Y. Enol Ethers Are Effective Monomers for Ring-Opening Metathesis Polymerization: Synthesis of Degradable and Depolymerizable Poly(2,3-Dihydrofuran). *J. Am. Chem. Soc.* **2020**, *142* (3), 1186–1189. https://doi.org/10.1021/jacs.9b11834.

(223) Feist, J. D.; Lee, D. C.; Xia, Y. A Versatile Approach for the Synthesis of Degradable Polymers via Controlled Ring-Opening Metathesis Copolymerization. *Nat. Chem.* **2022**, *14* (1), 53–58. https://doi.org/10.1038/s41557-021-00810-2.

(224) Fu, L.; Sui, X.; Crolais, A. E.; Gutekunst, W. R. Modular Approach to Degradable Acetal Polymers Using Cascade Enyne Metathesis Polymerization. *Angew. Chem. Int. Ed.* **2019**, *58* (44), 15726–15730. https://doi.org/10.1002/anie.201909172.

(225) Shieh, P.; Nguyen, H. V.-T.; Johnson, J. A. Tailored Silyl Ether Monomers Enable Backbone-Degradable Polynorbornene-Based Linear, Bottlebrush and Star Copolymers through ROMP. *Nat. Chem.* **2019**, *11* (12), 1124–1132. https://doi.org/10.1038/s41557-019-0352-4.

(226) Sathe, D.; Zhou, J.; Chen, H.; Su, H.-W.; Xie, W.; Hsu, T.-G.; Schrage, B. R.; Smith, T.; Ziegler, C. J.; Wang, J. Olefin Metathesis-Based Chemically Recyclable Polymers Enabled by Fused-Ring Monomers. *Nat. Chem.* **2021**, *13* (8), 743–750. https://doi.org/10.1038/s41557-021-00748-5.

(227) Chen, H.; Shi, Z.; Hsu, T.-G.; Wang, J. Overcoming the Low Driving Force in Forming Depolymerizable Polymers through Monomer Isomerization. *Angew. Chem. Int. Ed.* **2021**, *60* (48), 25493–25498. https://doi.org/10.1002/anie.202111181.

(228) Mulhearn, W. D.; Register, R. A. Synthesis of Narrow-Distribution, High-Molecular-Weight ROMP Polycyclopentene via Suppression of Acyclic Metathesis Side Reactions. *ACS Macro Lett.* **2017**, *6* (2), 112–116. https://doi.org/10.1021/acsmacrolett.6b00969.

(229) Neary, W. J.; Kennemur, J. G. Polypentenamer Renaissance: Challenges and Opportunities. *ACS Macro Lett.* **2019**, *8* (1), 46–56. https://doi.org/10.1021/acsmacrolett.8b00885.

(230) Ogawa, K. A.; Goetz, A. E.; Boydston, A. J. Metal-Free Ring-Opening Metathesis Polymerization. *J. Am. Chem. Soc.* **2015**, *137* (4), 1400–1403. https://doi.org/10.1021/ja512073m.

(231) Lu, P.; Kensy, V. K.; Tritt, R. L.; Seidenkranz, D. T.; Boydston, A. J. Metal-Free Ring-Opening Metathesis Polymerization: From Concept to Creation. *Acc. Chem. Res.* **2020**, *53* (10), 2325–2335. https://doi.org/10.1021/acs.accounts.0c00427.

Author Information

Sarah E. Blosch obtained her BS degree in Microbiology, with a minor in Chemistry, from the University of Oklahoma in 2009, after which she began working for Chevron Phillips Chemical Co. She returned to graduate school and in 2017 she obtained her MS in Macromolecular Science and Engineering under the tutelage of Prof. S. Richard Turner. She is currently working toward a PhD in Macromolecular Science and Engineering with Prof. John B. Matson, with an expected graduation date in the spring of 2022. Her research focuses on understanding the fundamentals of ring-opening metathesis polymerization to synthesize large, well-defined bottlebrush polymers.

Samantha Scannelli received her bachelor's degree in Biochemistry from Virginia Tech in 2017 and continues her studies as a graduate student under Professor Matson. Her work focuses on optimizing the conditions of ring-opening metathesis polymerization through monomer structure.

Mr. Alaboalirat received his undergraduate degree majoring in Chemistry in 2010 at Colorado School of Mines. Then, he moved to Saudi Aramco where he worked as a lab scientist in the research and development department in the crude oil emulsion group. In 2015, he moved to Virginia Tech to pursue a PhD in Macromolecular Science and Engineering under the supervision of Professor John Matson, with an expected graduation date of Summer 2022. His research focuses on the synthesis and characterization of bottlebrush polymers.

Professor Matson received his undergraduate degree majoring in Chemistry and German in 2004 at Washington University in St. Louis, performing undergraduate research with Professor Karen Wooley. He then moved to Caltech to pursue a PhD in the area of polymer synthesis with Professor Robert H. Grubbs.

He graduated in 2009 and moved to Northwestern University where he worked as a postdoctoral scholar on peptide-based biomaterials with Professor Sam Stupp. In 2012 he began his independent career at Virginia Tech in the Department of Chemistry, where he was promoted to Associate Professor in 2018 and Professor in 2021. His research focuses on macromolecular and supramolecular chemistry with applications in biology, medicine, and sustainability.